




Article

Earth Dam Design for Drinking Water Management and Flood Control: A Case Study

Bethy Merchán-Sanmartín ^{1,2,3}, Joselyn Aucapeña-Parrales ^{1,2}, Ricardo Alcívar-Redrován ^{1,2},
Paúl Carrión-Mero ^{1,2,*} , María Jaya-Montalvo ^{1,2,*}  and Mijail Arias-Hidalgo ^{1,4} 

- ¹ Facultad de Ingeniería Ciencias de la Tierra (FICT), ESPOL Polytechnic University, Escuela Superior Politécnica del Litoral, ESPOL, Campus Gustavo Galindo, Km. 30.5 Vía Perimetral, Guayaquil P.O. Box 09-01-5863, Ecuador; betgumer@espol.edu.ec (B.M.-S.); jaucapen@espol.edu.ec (J.A.-P.); raalciva@espol.edu.ec (R.A.-R.); mijedari@espol.edu.ec (M.A.-H.)
- ² Centro de Investigación y Proyectos Aplicados a las Ciencias de la Tierra (CIPAT), ESPOL Polytechnic University, Escuela Superior Politécnica del Litoral, ESPOL, Campus Gustavo Galindo, Km. 30.5 Vía Perimetral, Guayaquil P.O. Box 09-01-5863, Ecuador
- ³ Geo-Recursos y Aplicaciones (GIGA), ESPOL Polytechnic University, Escuela Superior Politécnica del Litoral, ESPOL, Campus Gustavo Galindo, Km. 30.5 Vía Perimetral, Guayaquil P.O. Box 09-01-5863, Ecuador
- ⁴ Centro del Agua y Desarrollo Sustentable (CADS), ESPOL Polytechnic University, Escuela Superior Politécnica del Litoral, ESPOL, Campus Gustavo Galindo, Km. 30.5 Vía Perimetral, Guayaquil P.O. Box 09-01-5863, Ecuador
- * Correspondence: pcarri@espol.edu.ec (P.C.-M.); mjaya@espol.edu.ec (M.J.-M.); Tel.: +593-99-826-5290 (P.C.-M.); +593-98-250-9363 (M.J.-M.)



Citation: Merchán-Sanmartín, B.; Aucapeña-Parrales, J.; Alcívar-Redrován, R.; Carrión-Mero, P.; Jaya-Montalvo, M.; Arias-Hidalgo, M. Earth Dam Design for Drinking Water Management and Flood Control: A Case Study. *Water* **2022**, *14*, 2029. <https://doi.org/10.3390/w14132029>

Academic Editor: Wenzhe Tang

Received: 26 April 2022

Accepted: 21 June 2022

Published: 24 June 2022

Publisher's Note: MDPI stays neutral with regard to jurisdictional claims in published maps and institutional affiliations.



Copyright: © 2022 by the authors. Licensee MDPI, Basel, Switzerland. This article is an open access article distributed under the terms and conditions of the Creative Commons Attribution (CC BY) license (<https://creativecommons.org/licenses/by/4.0/>).

Abstract: Water management for natural channels is a frequent challenge due to the inefficient usage of water resources. The 2030 Agenda of the United Nations (SDG 6 of sustainable development) focuses its attention on water and sanitation. The Sara Guerrero site, located in the Mocache municipality in Los Ríos province (Ecuador), has issues related to access to drinking water, flood control, and crop irrigation that affect 4300 people and 24,000 hectares. The river overflows throughout the rainy season (late December to early May), whereas there is a noticeable water shortage during the dry season. This project aims to design a multiple-use earth dam on the Vinces River, simulating the resulting flow in extreme cases due to its possible failure. Such a study implies the development of a contingency plan for the preservation of life. It considers (i) dam breach analysis and design, and (ii) hydraulic model development using the ArcMap and HEC-RAS software packages. The design includes a waterproofing system that controls possible leaks and a cymbal spillway, mainly for raw water collection. The generated model showed that the shorter the failure time, the higher the maximum output flow. Modelling revealed that four towns would be affected for a maximum of 31 h in extreme cases. This approach offers comprehensive management for this community with regards to the earth dam and flood control.

Keywords: earth dam; multiple-use dam; flooding; hydrological-hydraulic analysis

1. Introduction

The history of dam construction is as old as human civilization. The first indication of dam construction corresponds to ancient China (XII BCE), where their purpose was flood control [1]. These dams functioned by blocking water flow through civil infrastructure to create a temporary reservoir [2]. In general, the purposes of dams are: (i) to satisfy the supply of drinking and irrigation water in a controlled manner, (ii) to act as a flow regulator system in the event of droughts or floods, and (iii) to generate hydraulic energy. This all fits into a social, environmental, and economic vocation [3–8].

According to Singh [9], dams are classified in different ways, with size, types of materials used for construction, shape, purpose, and potential danger among the most relevant factors. Earth dams are the most common type of dam [10]; this typology has

strict requirements imposed on its design and construction [11]. The modern design of earth dams requires precise static and dynamic calculations based on a thorough analysis of stress–strain conditions. On the other hand, the design and construction of earthen dams and, in addition, rockfills, always result in a single structure that follows basic engineering principles [12].

In recent years, the widespread use of earthen dams for water retention has been determined by the possibility of: (i) using local soils and (ii) by the emergence of powerful mechanisms and the capability to build dams in difficult engineering–geological and seismic conditions [13]. However, it is essential to indicate that not all small dams are designed under engineering criteria and, mainly, their maintenance and management are not strictly regulated [14,15]. In general, dam safety management is directly related to the possibility of controlling and monitoring: (i) the current state and age of the construction and (ii) natural and geographical factors in operational planning. In the case of new earth dams (under design) or earth dams in operation, modelling techniques—as a complement to monitoring—open the way to predict their level of safety and risk [16,17].

From the point of view of structural risk, all dams carry a risk of failure [17]. However, earthen dams are less rigid and susceptible to failure [18]. Due to advances in hydraulic models, research on 2D models for flood risk management, including dam failures, has increased [19,20]. The Hydrologic Engineering Center’s River Analysis System (HEC-RAS) is a spatially fully-distributed event-based river hydraulic model designed to simulate: (i) one-dimensional steady flows, (ii) un-steady flows, (iii) sediment transport, (iv) water temperature, and (v) water quality [21]. In addition, the HEC-RAS can model both overtopping and pipeline failures of earth dams [22].

There are several examples of HEC-RAS software applications, for example, analysing possible dam failures and flood risk assessment in Crete (Greece), which is carried out using this tool and remote sensing data [23]. In addition, HEC-RAS software is used in the simulations of runoff-rainfall based on 2D hydrodynamics (Lombardy, Italy) [24], in the integration of the computational packages Soil and Water Assessment Tool (SWAT) and the HEC-RAS to simulate the rain-on-hydrodynamic 2D grid, allowing to quantify environmental flows [25], and in the evaluation of the risk of flooding of hydrographic basins (Ghamsar, Iran) combining the HEC-GeoRAS and HEC-RAS [26].

In rural areas of Ecuador such as the one characterised in this work, the problem of water and its management requires a series of actions to control it. In this context, interest arises in constructing a multiple-use dam in the rural sectors of the Mocache and Palenque cantons of the province of Los Ríos (Ecuador). The inhabitants of these sectors choose to dig wells to supply themselves with drinking water. In addition, it is estimated that 50,214 hectares that correspond to almost 90% of the territory of the Mocache Canton, where the study dam will be located, do not have any irrigation and are occupied by crops of corn, cocoa, African palm, and other minor crops, which implies a deficit in irrigation in the province [27].

The aim of the present study is: (a) to design a multiple-use earth dam on the Vinces River using HEC-RAS and HEC-GeoRAS software; and (b) to perform specific hydraulic calculations for the dam failure analysis, simulating the resulting flow in extreme cases due to its possible failure, which determines a contingency plan for the preservation of life.

2. Study Area

The study area is located in the central part of Ecuador, in the Los Ríos province of the coastal region of the country (Figure 1a,b). The province of Los Ríos constitutes of the most significant production of export bananas in monoculture, with 2,368,526.14 tons of bananas produced in 2019 [28]. According to INEC data [29], in its last census, the province’s total population is 778,115.0, and almost 65% of the population lives in the rural sector. In addition, the region has one of the main river systems in Ecuador, known as the “Guayas River Basin”. The system covers 10 provinces (Bolívar, Cañar, Cotopaxi, Chimborazo, Guayas, Los Ríos, Manabí, Tungurahua, Santo Domingo de los Tsachilas,

Santa Elena), the drainage network of which is born in the foothills of the western Andes Mountain range and flows into the Gulf of Guayaquil.

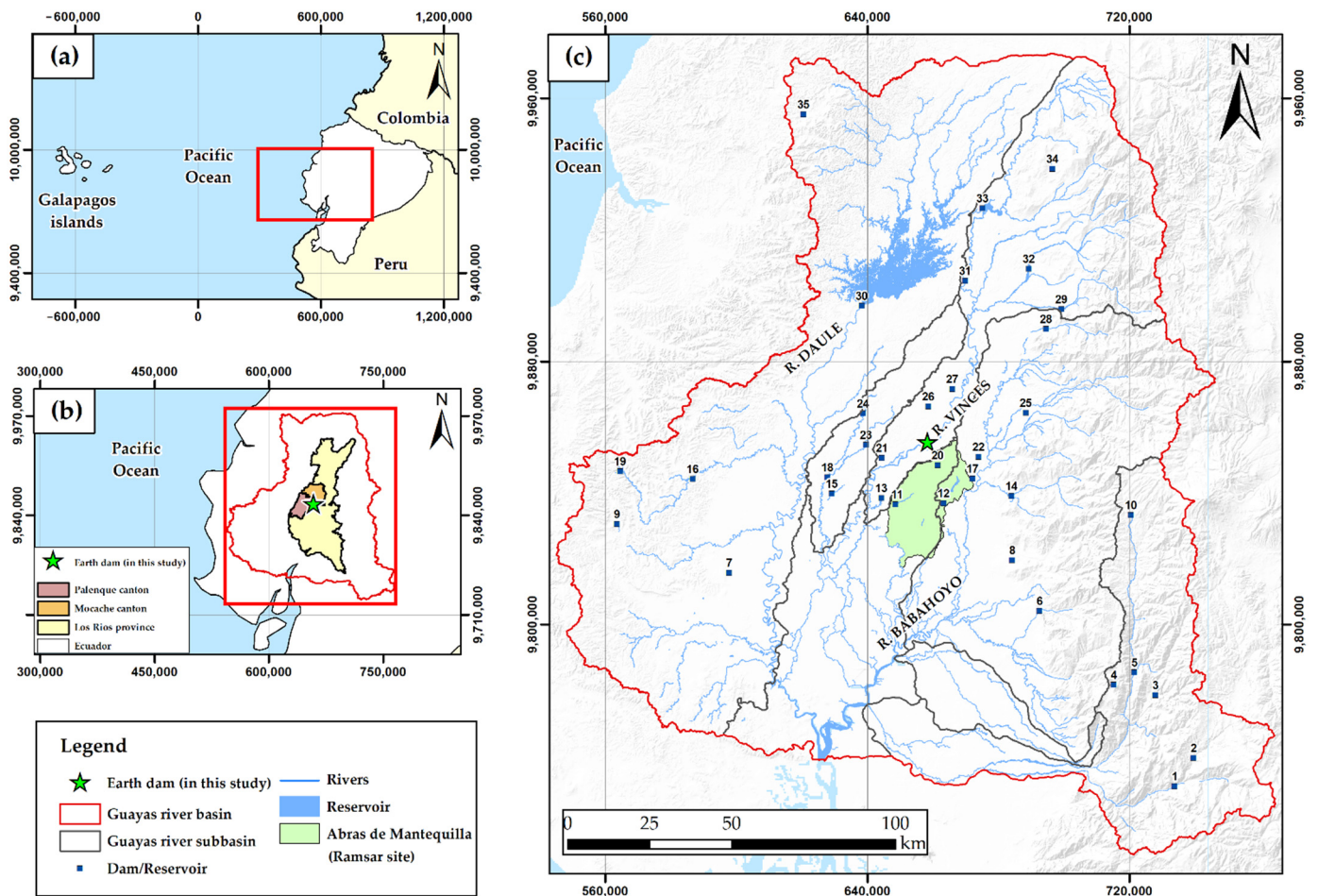


Figure 1. Study area location: (a,b) Los Ríos province and main cantons within the earth dam zone proposed in the present study; (c) Guayas river basin, Guayas river subbasin and Hydraulic works or infrastructure (reservoirs and dams) location in the area by [32], 1: Guashán, 2: Chanconvento, 3: Coco, 4: Chillanes, 5: Pangor Bucay, 6: Cristal, 7: Bufay, 8: Pita, 9: Paján, 10: Salimoya, 11: Chojampe, 12: Puebloviejo, 13: Estero Lechugal, 14: Sibimbe, 15: La Angostura, 16: Pajamayo, 17: Aguacatal, 18: Macul 2, 19: Conguineal, 20: Chojampe 2, 21: Mangas-Saibas, 22: Lechugal 2, 23: Maculillo, 24: Macul 1, 25: Suquibi, 26: Garzas, 27: Mocache, 28: Calope, 29: San Pablo, 30: Daule-Peripa, 31: Quevedo, 32: Quindigua, 33: Baba, 34: Bimbe, 35: Flavio Alfaro.

The study’s multiple-use earth dam is located in the lower-central basin of the Guayas River between the cantons of Palenque and Mocache, about 300 km southwest of Quito and about 45 km from the Daule-Peripa reservoir (Figure 1c). In addition, the basin contains the “Abras de Mantequilla” wetland reserve, catalogued as a “continental wetland” designated as Wetlands of International Importance (Ramsar Sites) in 2000 [30,31].

3. Materials and Methods

The methodology adopted in this study is divided into two phases (Figure 2): (i) phase I, dam breach analysis and design; and (ii) phase II, hydraulic model development.

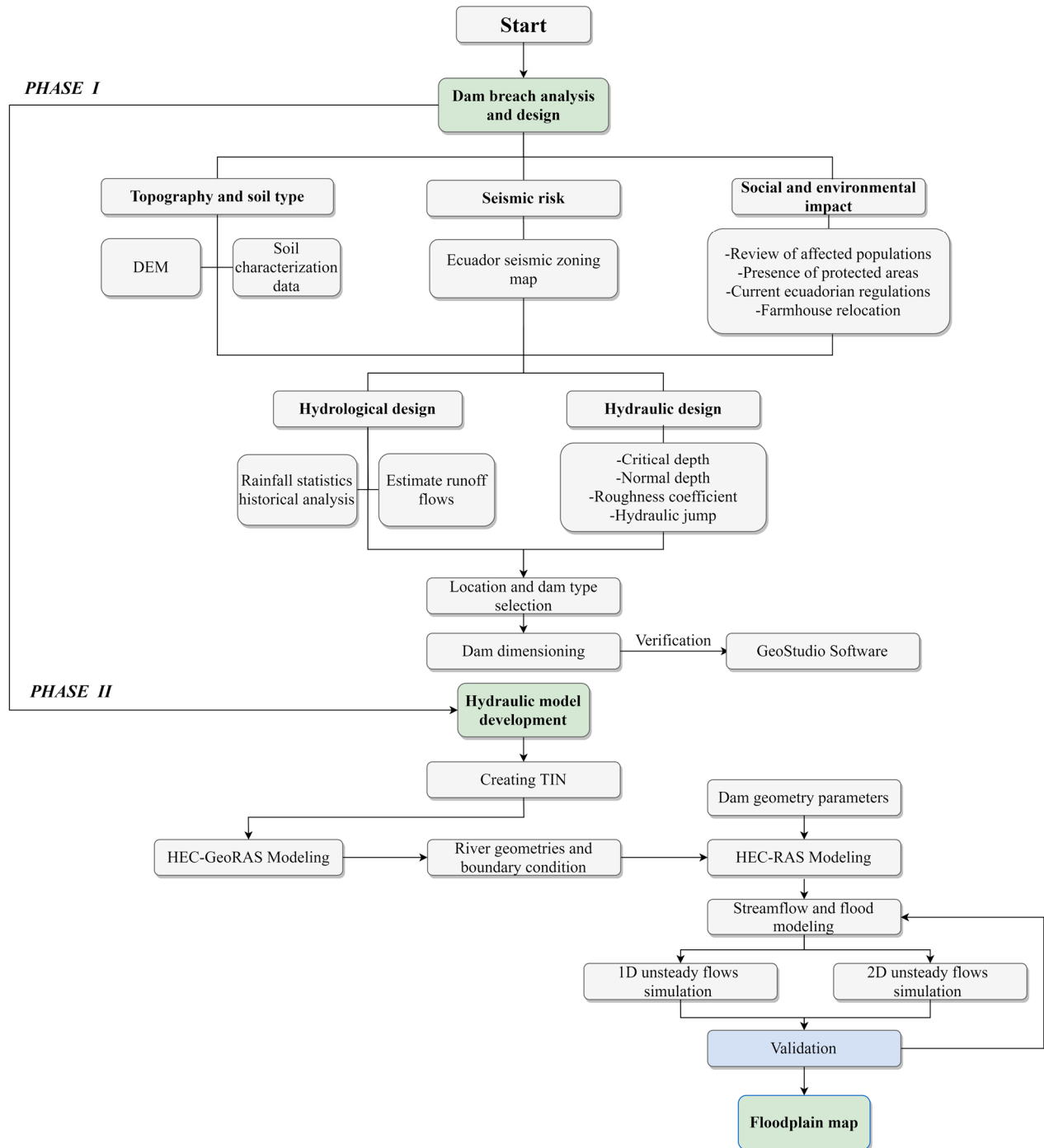


Figure 2. Scheme of the methodology followed in this study.

3.1. Stage I: Dam Breach Analysis and Design

For the dam dimensioning, it was necessary to determine, in the first phase, the most convenient place and type of dam for the study area. In this context, five aspects were analyzed: topography and soil type, seismic risk, social and environmental impact, hydrological design, and hydraulic design.

3.1.1. Topography and Soil Type

The topographic data processing in raster format was carried out in conjunction with the bathymetry of the Vines River to obtain a resolution equal to that of the topographic Digital Elevation Model (DEM) of the Guayas River basin (cell size field: 12.5×12.5 m) [33]. In the soil typology, the material used in the dam (characterization of soils) and accessibility of material (location of quarries closest to the study area) was analysed. In addition, the influence of geological characteristics (local geological, geological contact points, and presence of geological faults in the cartography of the sector) [34,35] and land uses were evaluated.

3.1.2. Seismic Risk

For the characterization of the seismic hazard, the Z value (maximum rock acceleration expected for the design earthquake) of the study area was identified based on the seismic zoning map of Ecuador available in the NEC chapter Seismic Hazard–earthquake-resistant design [36].

3.1.3. Social and Environmental Impact

It was necessary to evaluate the potential implantation areas' economic, social, environmental, and legal characteristics to identify this type of work's advantages, disadvantages, effects, and contributions. In this stage, land cost data were collected through open interviews with the local government. In the towns near the dam, implementation alternatives were identified, which would involve a compensation process for the damages caused by relocation processes and the possible acquisition of new territory for those affected. In the environmental aspect, the presence of protected areas, landscape impact, dust, erosion, loss of vegetation, and earth movements were evaluated [37]. According to these criteria, an environmental mitigation plan was developed through the environmental impact identification matrix proposed by Conesa [38]. Finally, the current Ecuadorian regulations, construction, environmental, hydraulic, seismic, and geotechnical requirements of the project were reviewed in the legal framework.

3.1.4. Hydrological Design

The analysis of precipitation extremes was carried out using the flow values of the hydrological yearbooks of the National Institute of Meteorology and Hydrology (INAMHI acronym in Spanish) [35]. Specifically, the information of the meteorologic stations with codes H348 (Vinces) and H0347 (Quevedo) between the years 1964–2013 and 1962–2015 belong to the study basin [39]. As the rain data records in most of the meteorological stations of Ecuador are incomplete, it was necessary to analyse extremes to determine the design flow. Therefore, through the series of annual maximum daily flows (m^3/s), various return periods (100, 200, and 500 years) were used. In addition, five theoretical probability distributions, such as Gumbel [40], Log-Normal [41], Pearson III [42], Log Pearson III [43], Ln Pearson III [44], and the Kolmogorov-Smirnov test [45], were taken into account to determine the best-fitting model.

3.1.5. Hydraulic Design

A dam is a structure or control surface and commonly causes a hydraulic jump effect upstream of the spillway. It is thus necessary to know its length and its impact on the riverbed, and, importantly, whether it can affect nearby populations in case of a breakage. Therefore, specific hydraulic data calculations were performed to determine the key factors. Equation (S1) (Supplementary Materials) was used following the Chugaev method [46]. The equation depends on the determination of Z_c and Z_i (section factor at a critical point and point 'i'), obtained through Equations (S2) and (S3), respectively (Supplementary Materials). With these data, it was possible to find the value of M (Chugaev factor), which is given by expression (S4) (Supplementary Materials). The procedure was carried out for three different locations within the study area: Alternative A (Mocache Sector), Alternative B (Sara Guerrero Sector), and Alternative C (La Libertad Sector).

The Bakhmeteff variant [47] was used to determine the normal depth, employing Equations (S5)–(S8) (Supplementary Materials). The n is the Manning coefficient for the section to be analysed, estimated, and corrected using the Cowan method [48]. The Cowan method considers different factors for selecting the Manning roughness coefficient as shown in Equation (1), where n_b represents the base value of n for the channel and the different n_i factors are correction factors.

$$n = (n_b + n_1 + n_2 + n_3 + n_4) \times m, \quad (1)$$

Hence:

n_1 : Effect of bottom irregularities and scour potential.

n_2 : Variations in the size and shape of channel cross-sections.

n_3 : Presence of obstructions.

n_4 : Vegetation and flow conditions.

m : Correction factor for channel meanders.

The procedure to determine the roughness coefficient along the river consisted of designating cross-sections every 10 m. The United States Department of Agriculture [49] was taken to establish soil characteristics. With these parameters, base values of the roughness coefficient were designated [50].

In addition, the predictor–corrector method (Equation (S9), Supplementary Materials) was used to estimate the length of the backwater curve. Finally, the Manning’s coefficient was determined, and the estimated depth was compared to obtain the normal depth in the three alternatives (the data required for the normal depth are detailed in Table S1, Supplementary Materials).

3.1.6. Location and Dam Type Selection

Based on the five aspects described, eight direct incidence parameters were defined to select the final location of the dam to be designed. The quantifying parameters are: (i) Seismic Risk, (ii) Environmental Impact, (iii) Social Impact, (iv) Geological Faults, (v) Soil Type, (vi) Topography, (vii) Hydraulics, and (viii) Economy. The 5-point Likert scale [51] was used in the selection process. The categories of the Likert scale from lowest to highest are one is “totally unfavorable”, two is “certainly unfavorable”, three is “neutral or indifferent”, four is “certainly favorable”, and five is “totally favorable”, depending on how high or low a specific criterion was met. For instance, for topography, if the area is too plain or wide, it is not recommendable to select this place because of the large volumes involved to close the dam and budget constraints. After the corresponding weights for each criterion, the alternative with the highest score was selected. The parameters have the same weight to avoid bias in the results and to allow a holistic view of the quantifying parameters. Due to geotechnical conditions, two possible materials were established for the dam type selection, namely concrete or earth-fill. The latter was chosen for the design due to the geomorphology, for material availability reasons, and because its associated seismic vulnerability is generally low, both under static and dynamic load conditions [52].

3.1.7. Dam Dimensioning

The dam was dimensioned with the established hydrological, hydraulic, topographic, and geological parameters using equations proposed in the literature [53]. Therefore, it was necessary to carry out specific calculations for the correct dimensioning of the dam, detailed in (Supplementary Materials). To calculate the height of the dam, we start with the definition of the levels to be used: Ordinary High Water Level (NAMO acronym in Spanish) with which the valuable capacity of the reservoir is designed, Extraordinary Maximum Water Level (NAME acronym in Spanish), and bed level (NSC acronym in Spanish).

Based on the SP 38.13330.2012 standard cited by Sandoval [53], the dam’s height considers a shelter above the static level of the reservoir (Equation (S10)); Equation (S11) was used to determine the wave drag superelevation. Finally, Equation (S12)—suggested by

Buldeya [54]—and the roughness coefficient through Equation (S13) (Supplementary Materials) were used to estimate the bearing height. Then, the parameters (see Table S2, Supplementary Materials) were calculated depending on the height and dimensions.

A thick-walled spillway type WES (Waterways Experiment Station) was designed. The US Army Corps of Engineers [55] established this weir to unify various types of profiles commonly used in non-vacuum thick-walled weirs. Although this organization made it a standard, the original considerations for this design were proposed by the United States Bureau of Reclamation (USBR) [56]. Initially, the estimated discharge on the crest of the spillway was calculated according to Equation (2).

$$Q = C_0 \times \sqrt{2g} \times L \times H_0^{3/2}, \quad (2)$$

where C_0 is the discharge coefficient, g is gravity, L is the effective length of the crest (m), and H_0 is the total load on the crest (m). However, the C_0 , in turn, depends on five factors, as indicated in Equation (S18) (The Supplementary Materials presents details of the discharge coefficient).

3.2. Stage II: Hydraulic Model Development

In stage II, the simulation is performed in 1D unsteady flows and 2D unsteady flows to perform the hydraulic modelling of dam failure. It begins with the pre-processing stage that includes the creation of the Triangular Irregular Network (TIN) of the study area through 3D Analyst tools of the DEM created in phase II. Then, the input data is created through the HEC-GeoRAS software, a GIS extension. These data are the cross-sections, hydraulic structures (e.g., bridges), riverbanks, and other geometric characteristics of the fluvial channel, which will be exported to the HEC-RAS software developed by the US Army Corps of Engineers (USACE) used in several dam failure analysis studies [19,22,23,57].

Different scenarios were considered for the fracture analysis; a trapezoidal fracture was modelled according to what was proposed by Froehlich (1995) [58] and Froehlich (2008) [59]. Within this scenario, a partial and a total rupture were considered. In each event, the avenue change due to bridges upstream and downstream of the dam was evaluated. Once the bridges were identified, the software modelled the bridges with the corresponding slab, piers, and abutments values.

In HEC-RAS, the “Inline structure” tool was used to enter the geometry of the dam. The “ogee” option was considered for the structure, and the “breach beam structure” was chosen to simulate the structure’s failure. Once the parameters of the geometry of the terrain and the structure were inserted, the boundary conditions (BC lines) were entered for unsteady or non-permanent flows. In this analysis, the boundary conditions were defined by the flow hydrograph (Figure 3) at the beginning of the cross-sections. The flow hydrograph was calculated as a synthetic hydrograph using Microsoft Excel by entering rainfall and catchment area data.

On the other hand, the bottom slope (normal depth) was chosen as a downstream boundary condition. After the 1D unsteady flow analysis, for the 2D unsteady flow modelling, which is floodplain mapping, the TIN of the study area was imported from ArcGIS. A 2D area of all the land that could be affected downstream of the dam was created. Two boundary conditions were placed—one at the dam’s location, and another at the end of the area that was estimated to possibly be affected in the analysis. As in the 1D unsteady flows simulation, the hydrograph was entered at the first BC line, and at the last line, a normal slope was entered as the downstream boundary condition.

When using the HEC-RAS software for dam failure analysis where the type of flow is rapidly variable, it is necessary to take several considerations to make the model more stable, such as (i) decreasing the distance between cross-sections, (ii) reducing the calculation interval, and (iii) apply theta weighting factor. This weighting factor is used in the transient mode, whose value ranges from 0.6 to 1, where 1 provides the most stable results possible [60,61]. In this study, the starting value of 1 was used [22], and the value of theta was experimented with until it reached 0.6, finally adopting the value of 1.

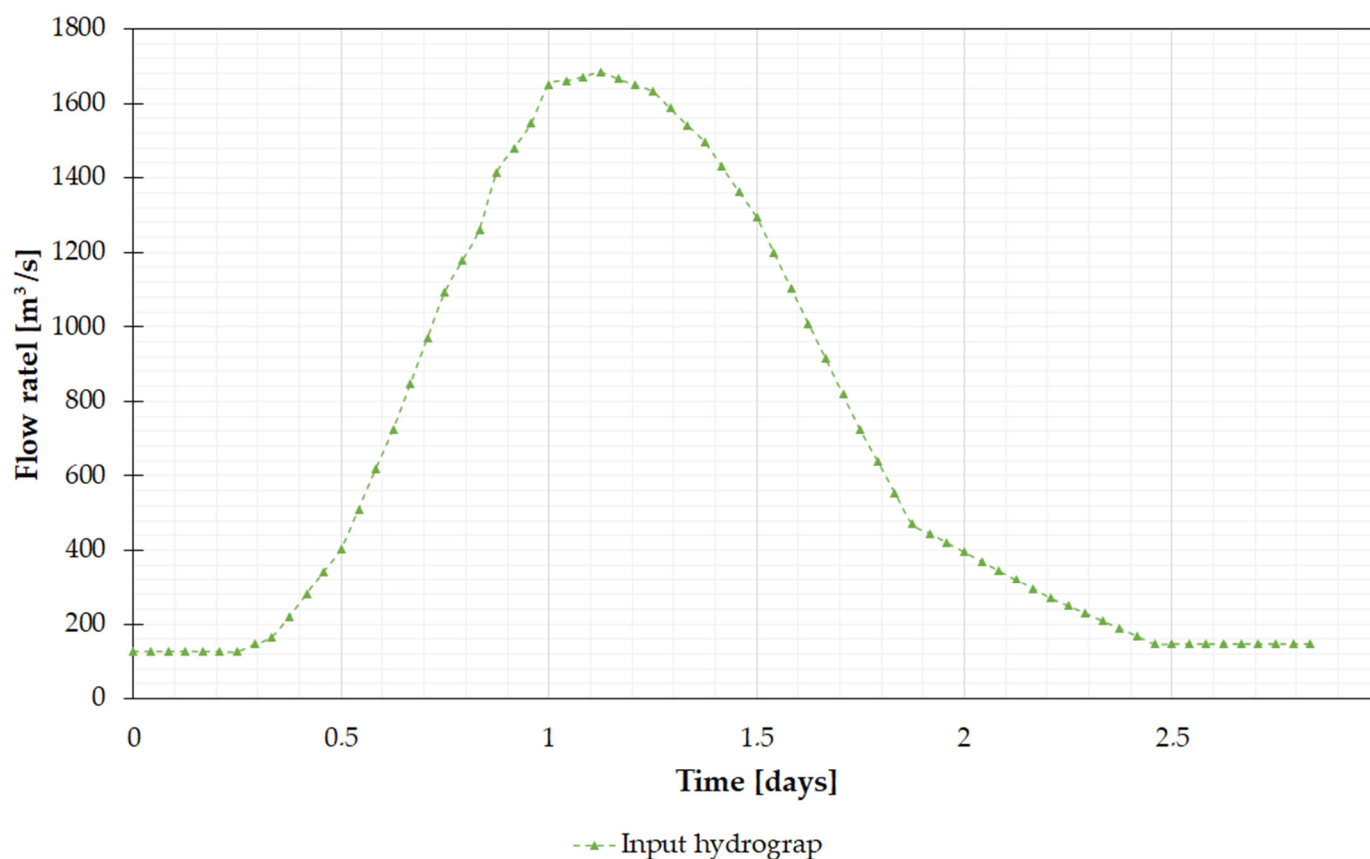


Figure 3. Design hydrograph as at boundary condition.

4. Results and Discussion

4.1. Dam Breach Analysis and Design

4.1.1. Topography and Soil Type

In general, the topographic environment of the project is characterized by low slopes between 2% and 3%. The terrain is flat with very gentle mountainous relief (Figure 4). The area of interest of the proposed alternatives in the Vinces riverbed (Figure 4b) is very flat, with a relief that varies from approximately 0 to 60 m.

Alluvial deposits (Figure 5) prevail around alternatives 1, 2, and 3, characterized as detrital materials transported by the Vinces River and deposited along its plain. They are generally composed of sand, clay, and gravel. In addition, deposits of undifferentiated alluvial terraces are formed in the area, made up of poorly consolidated clays and sands. These sediments are used as a base for the different crops in the sector. The alluvial deposits rest on a volcanic basement from the Late Cretaceous (Piñón formation), which does not outcrop in the geological environment of the study area. Two geological fault lines with a NE–SW trend can be seen, which are not dangerous to the dam’s area. Regarding soil typology, there is a more significant predominance of Entisols, Mollisols, Alfisols, Inceptisols, and Vertisols in the area.

4.1.2. Seismic Risk

According to the NEC [36], for the province of Los Ríos in the Quevedo and Vinces cantons, the Z factor is 0.35. Therefore, the study area is located in seismic zone IV. Consequently, the dam’s location implies a high seismic hazard, which consequently means analysing the behaviour of large structures (e.g., dams) during an earthquake of a significant magnitude.

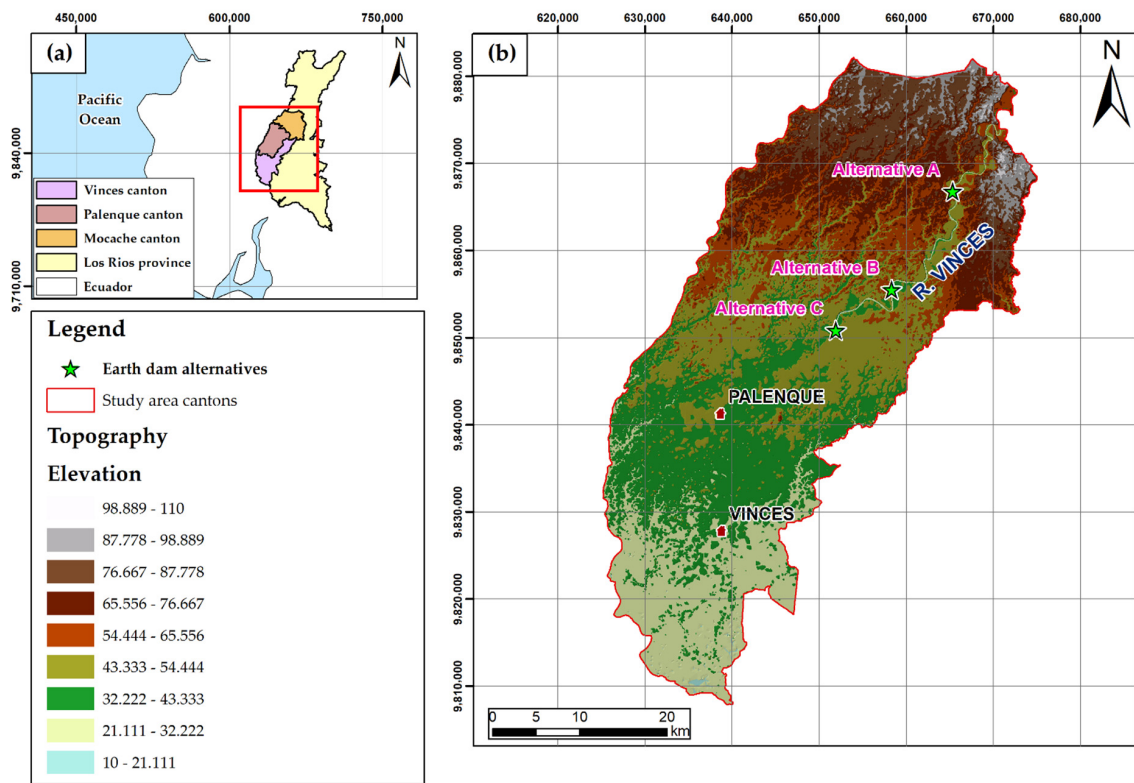


Figure 4. (a) Location of the main cantons in the study area; (b) The general topography of the study area with the location of the three alternative locations of the earthen dams.

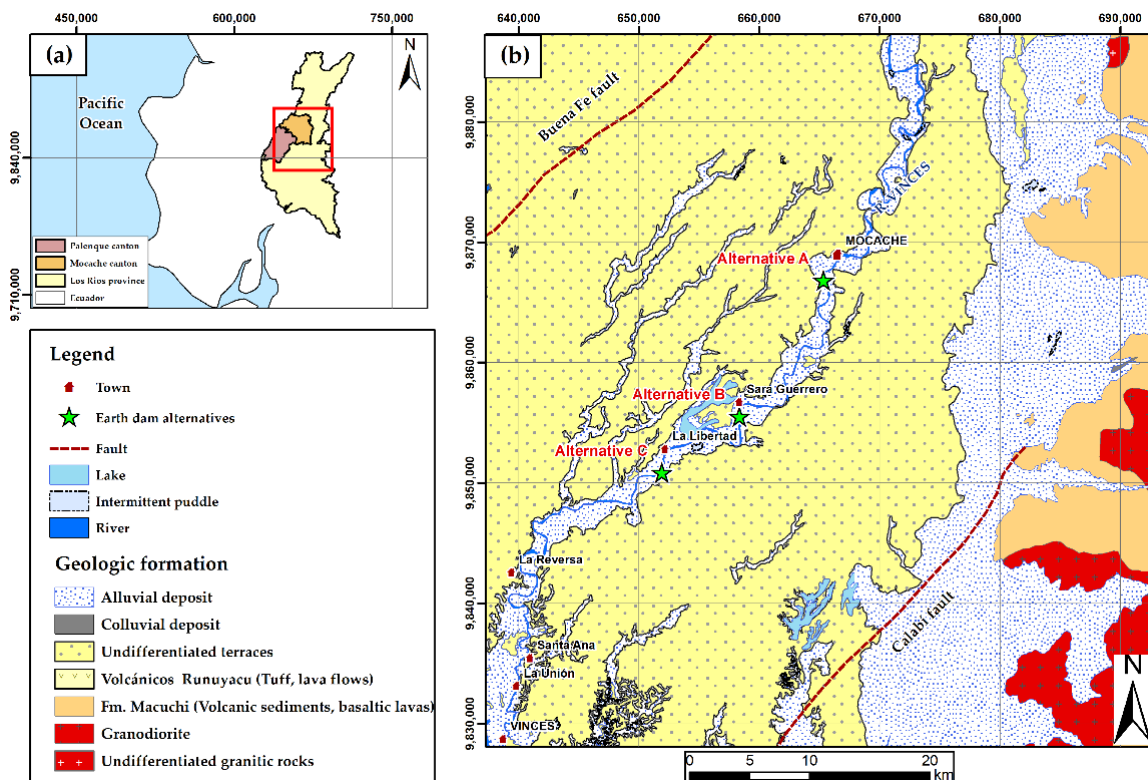


Figure 5. Earth dam alternatives setting. (a) Geographic setting in the present study; (b) Geological setting with the location of the three alternative locations of the earthen dams [62,63].

4.1.3. Social and Environmental Impact

The construction of a dam involves the relocation of villages, towns, and possible compensation [64,65]. Despite this, its construction contributes to improving the quality of life of the populations near the area (e.g., agriculture). The options chosen to implement the reservoir are close to different towns and the possible acquisition of new territory for those affected (Table 1).

Table 1. The population that is possibly affected by the implementation of the dam in each alternative option.

Alternatives	Towns	Population	Total
A	Las Campanas	480	1827
	La Porfia	320	
	Emperatriz	387	
	Buena Aventura	340	
	Gramalotillo	300	
B	Sara Guerrero	487	487
C	La Libertad	526	526
Total		2840	

Additionally, the assessment of the identified environmental impacts and the proposal for environmental mitigation are shown in Tables S3 and S4, respectively. The assessment of the impact in Table S3 in terms of their relevance varies between 4 and 81 points. The presence of fine particles generated by both the movement of loose earth and the cement used for concrete is the most critical impact because it is immediate. Additionally, the environmental impact matrix considered effects on fauna and flora. In Ecuador, bio-aquatic resources are regulated in the Los Ríos province; a seasonal ban was established for all water species between January 10 and March 10 every year. In the report carried out by Revelo et al. [66], a total of 3772 fish specimens were analysed, implying up to 16 species. Given this crucial situation, a fish passage was included in the dam design phase.

4.1.4. Hydrological Design

Table 2 shows the results obtained for flows using probabilistic methods and return periods of 100, 200, and 500 years, according to rainfall data from the Quevedo and Vinces stations. The Vinces hydrological station was chosen because its meteorological information does not have gaps (Table 2) [39]. The Pearson III distribution is the best fit method (in bold in Table 3, pink in Figure 6), while the other distributions do not satisfy the Kolmogorov–Smirnov test [45]. Similar to the present study, the Log Pearson III method was used in the Himalayan river basin of Nepal in 2020 [67].

4.1.5. Hydraulic Design

Table 4 shows the values of the normal and critical depth prior to estimate the resulting water surface. These values are necessary to calculate the length of backwater curve due to the dam and whether it affected nearby towns.

4.1.6. Location and Dam Type Selection

Regarding the methodology applied to determine solutions, the five-point Likert scale [51] was used to select the best alternative for the implantation of the dam. This scale is a qualitative or semi-quantitative method used to measure attributes based on opinions/valuations/ratings [68]. It is used for the sustainable management of water resources [69–71] in the water domain and engineering projects [72–74]. Using this tool in the dam design allows for an integral vision of the parameters of direct incidence in the dam's location and to choose the best option considering both technical, social, and environmental aspects; in this case, the alternative B was selected (Table 5).

Table 2. Flows obtained by probabilistic methods.

Flows along the Vinces River [m ³ /s]				
Station: Quevedo				
Return period [years]	Gumbel	GEV I	Log Normal	Pearson III
100	549.7	481.3	705.5	511.6
200	600.3	527.3	811.1	568.2
500	667.0	588.0	960.4	643.9
Station: Vinces				
Return period [years]	Gumbel	GEV I	Log Normal	Pearson III
100	1326.0	1225.1	1187.1	1252.3
200	1396.7	1288.5	1230.4	1323.7
500	1489.9	1372.0	1284.8	1418.4

Table 3. Kolmogorov–Smirnov test at the Vinces station.

	Gumbel	GEV I	Log Normal	Pearson III
Δ_{max}^1	4.5%	5.0%	13.1%	0.6%
Δ_0^2	12%			
Fit	Accept	Accept	Reject	Accept

¹ Δ_{max} = the most significant absolute difference between the observed and theoretical cumulative frequency;
² Δ_0 = the critical level of the contrast.

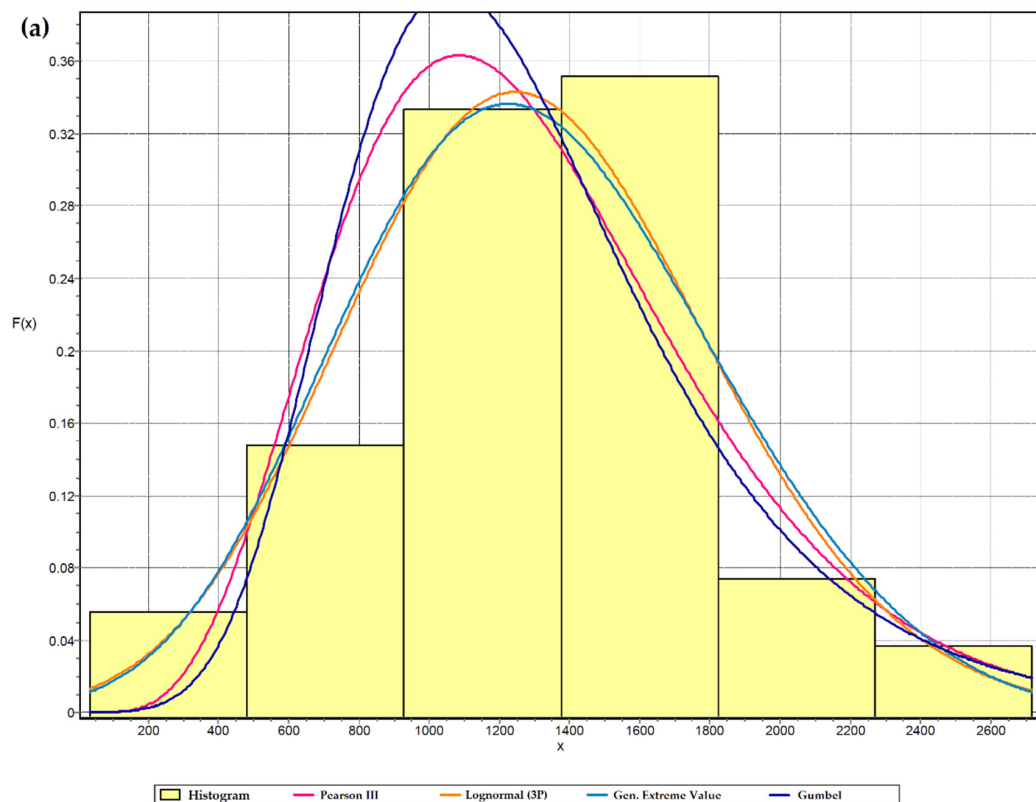


Figure 6. Cont.

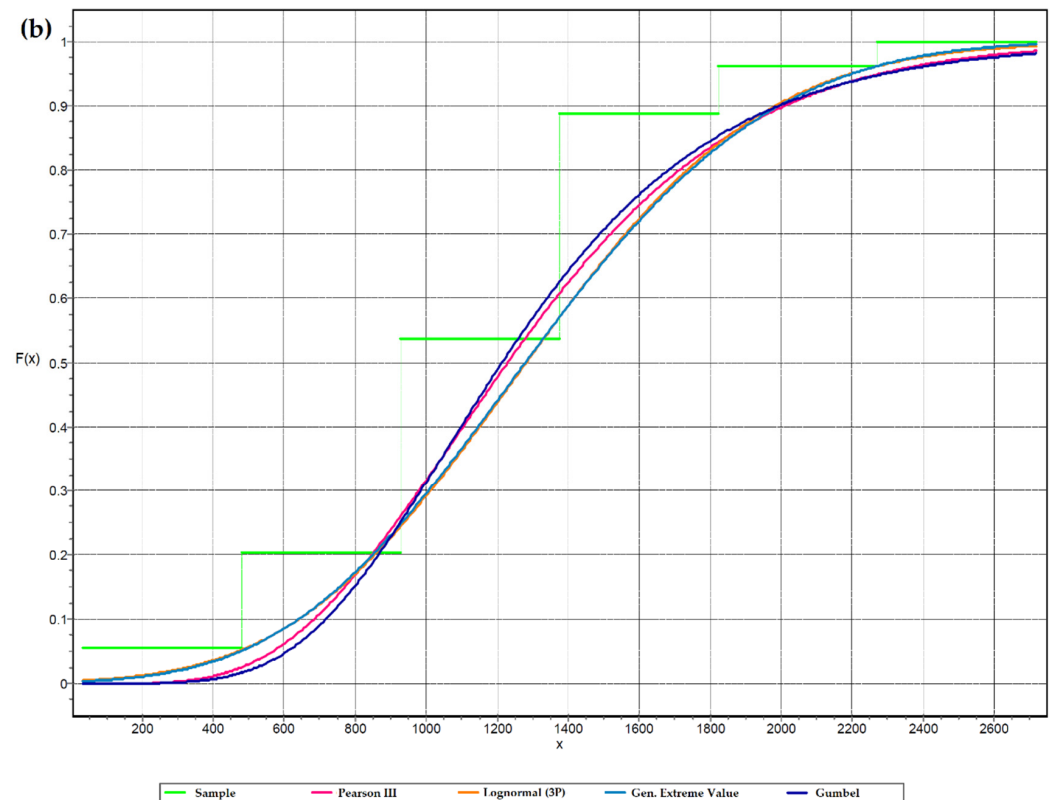


Figure 6. (a) Probability distribution functions (PDF) and (b) cumulative distribution functions (CDF) at the Vincennes station.

Table 4. Critical depth (Y_c) and Normal depth (Y_n) for alternatives A, B, and C.

Alternative	Y_c [m]	Y_n [m]
A	2.004	16.253
B	4.201	16.304
C	2.581	15.674

The alternative B obtained 25 points because its hydraulic backwater does not cause significant damage to the populations upstream of the dam implementation. In addition, it is located 90 min from the “Santa Lucía” quarry, where the aggregates for the construction of the dam will be provided. The location is ideal because population displacement is minimal compared to the other alternatives. It has a flat terrain, semi-mountainous regions, and broad valleys. The dam material will be mixed due to favourable soil conditions for an earthen dam. However, it is necessary to implement concrete dikes and the respective foundation of the hydraulic structure. Table 6 presents the main characteristics of alternative B.

Table 7 shows the steps performed in the predictor–corrector method. The length of the hydraulic pool of alternative B is 15.5 km, which does not affect nearby towns.

4.1.7. Dam Dimensioning

Table 8 shows the initial values for the hydraulic analysis in HEC-RAS where cross sections were established every 10 m and the flow obtained in the hydrological study was used, with a return period of 100 years for the hydraulic analysis.

Table 5. Results of the assessment using the Likert scale for alternatives A, B, and C.

Quantifying Parameters	Score					
	5	4	3	2	1	
Alternative A	Seismic risk		x			
	Environmental impact			x		
	Social impact				x	
	Geological faults			x		
	Soil type			x		
	Topography		x			
	Hydraulics					x
	Economy				x	
Total			20			
Alternative B	Seismic risk				x	
	Environmental impact			x		
	Social impact			x		
	Geological faults			x		
	Soil type			x		
	Topography		x			
	Hydraulics		x			
	Economy			x		
Total			25			
Alternative C	Seismic risk				x	
	Environmental impact			x		
	Social impact		x			
	Geological faults			x		
	Soil type			x		
	Topography		x			
	Hydraulics			x		
	Economy					x
Total			24			

Table 6. Main characteristics of the alternative chosen in the study.

Alternative B	
Dam location	Easting: 658,327/Northing: 9,855,587 (UTM WGS 84/17M)
Dam material	Earth with compacted core
Type of soil in the area	It is superficially formed by alluvial deposits, undifferentiated terraces, coarse sand, and clay.
Environmental impact	There are no protected areas within the area; with a prevention and mitigation plan, the impact caused by construction methods is reduced.
Economic impact	The benefit covers 44 thousand hectares of cultivation, and 200 jobs are generated.
Social impact	There are no large populations affected by displacement.

Table 7. Backwater Length of Alternative B.

Alternative	y [m]	y + $\Delta y/2$ [m]	Area [m ²]	P [m]	T [m]	Num/h ₁	Den/h ₁	Δ_x [m]	x [m]
B	20.00								0
		19.75	1446.02	112.91	99.99	0.000168	0.994713	2951.737	
	19.50								2951.737
		19.25	1396.39	111.15	98.55	0.000125	0.994214	3969.896	
	19.00								6921.633
		18.75	1347.47	109.40	97.11	0.0000765	0.993655	6494.358	
	18.50								13,415.99
		18.25	1299.28	107.65	95.67	0.0000215	0.993027	23084.6	
	18.00								36,500.59
		17.75	1251.80	105.90	94.23	−0.000041	0.99232	−12176.5	
	17.50								24,324.09
		17.25	1205.05	104.15	92.80	−0.00011	0.991522	−4448.7	
	17.00								19,875.39
		16.75	1159.01	102.40	91.36	−0.00019	0.990619	−2580.15	
	16.50								17,295.24
	16.25	1113.69	100.65	89.92	−0.00028	0.989593	−1742.14		
16.00								15,553.09	

Table 8. Initial conditions for hydraulic analysis.

Parameters	Value
River length	163,650.00 [m]
Slope	0.001
Cross sections	10 m
Flow (return period = 100 years)	1252.30 [m ³ /s]

The failure parameters estimation was modelled using a trapezoidal rupture by the Froehlich (1995) [58] and Froehlich (2008) [59] method, which is directly related to the height of the rupture, the volume of the dam, the lateral slope of the failure, and the failure mode factor. The use of these factors is the reason why the results are more conservative compared to the Macdonald and Langridge–Monopolis [75], Evans [76], USBR [56], or Kirkpatrick [77] methods. However, the two methods have been used in other dam studies, such as the Froehlich equation (2008) in the Hidkal dam in India, to analyze piping and overtopping failure [78]. In addition, they were used in the 2D unsteady simulation analysis in the Gidabo dam in Ethiopia [79] that used the methods of Froehlich (1995, 2008) [58,59] and Macdonald and Langridge–Monopolis [75], concluding that the Froehlich equations (1995) [58] are the most suitable method for simulations in unsteady flow.

In order to take into account, the failure of the dam at different times, failure simulation was performed in two scenarios: instantaneous (scenario A) (Figure 7) and total (scenario B) (Figure 8). Table 9 shows the water levels and maximum flows reached by the flow at the precise moment of the dam failure.

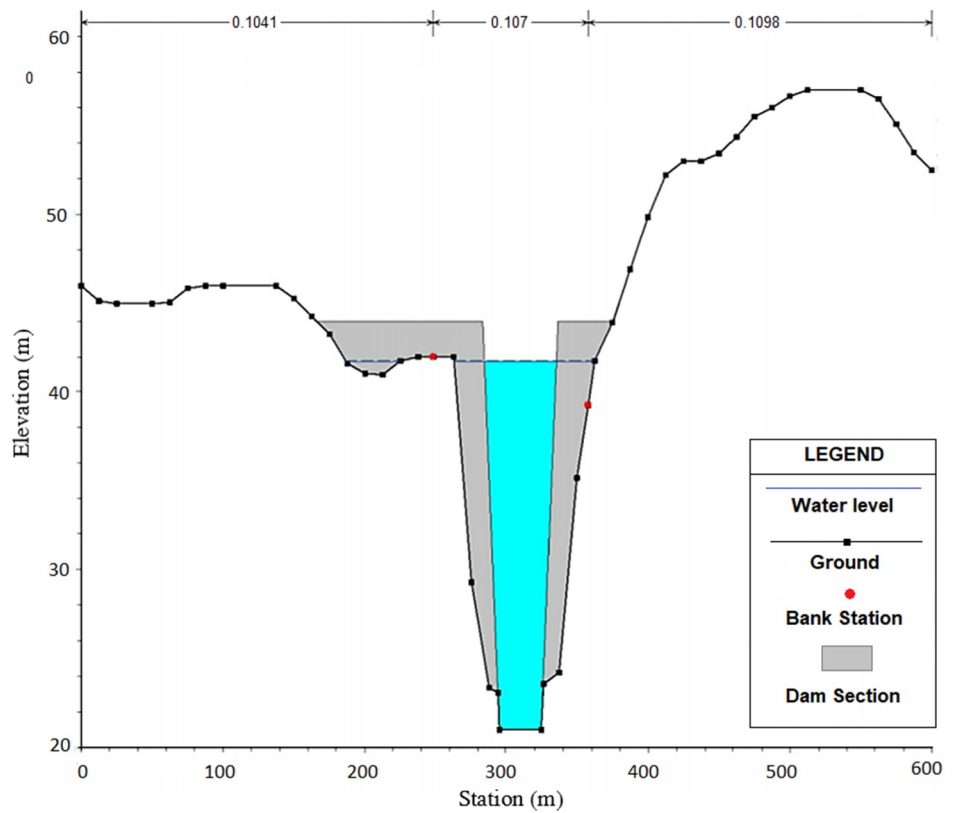


Figure 7. Failure scenario A at T = 1.03 h.

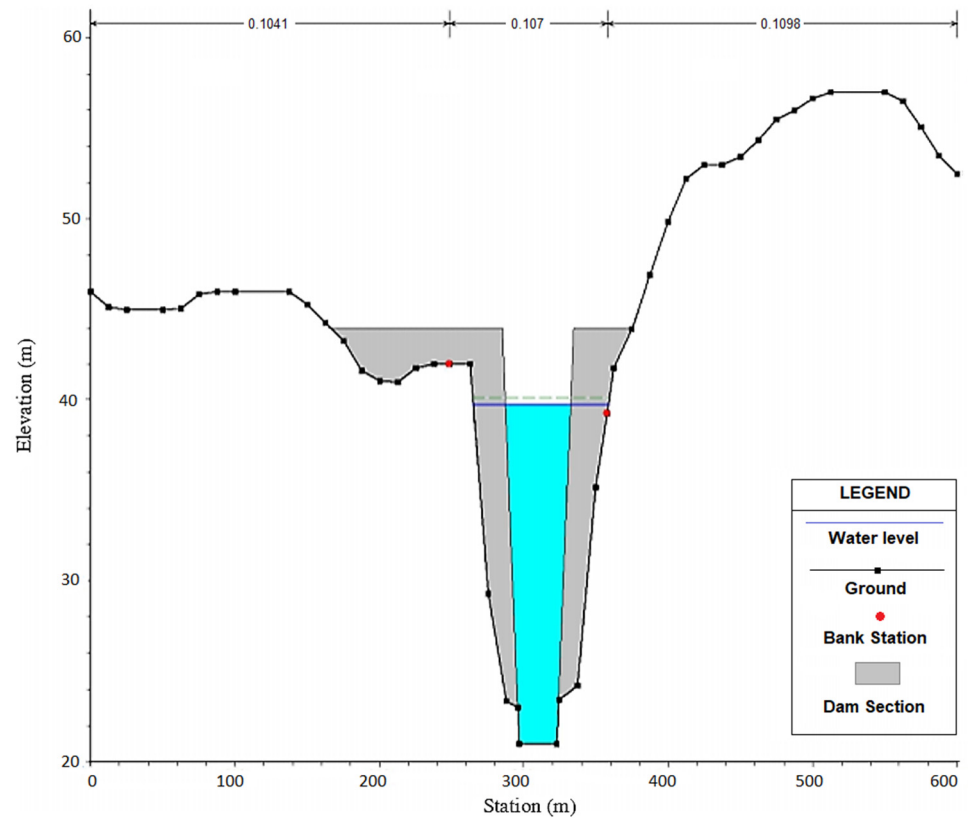


Figure 8. Failure scenario B at T = 68 h.

Table 9. Maximum levels and flows for the different scenarios of dam failure.

Type of Failure	Level [m]	Flow [m ³ /s]
Instant Time: 1.03 h	43.79	2901
Total Time: 68 h	44.77	1400

Additionally, the hydrograph Flow vs. Time of scenario A (Figure 9) and scenario B (Figure 10) and the longitudinal profile of the river were made (Figure 11). In the instantaneous failure (Figure 9), it is observed how the level both upstream and downstream begin to fluctuate sharply before converging at level 40. At that instant, the water reservoir and the body of water after the dam can be considered a single body. Thus, producing an effect of communicating vessels, the level becomes uniform. Upon reaching elevation 44, it seeks balance in its energy, completely covering the remnant dam dike. The speed of flow change occurs suddenly, reaching its peak at the moment in which the bodies of water come together. After that, the flow decreases until it reaches a continuous value.

In the total failure (Figure 10), it is observed that the level of both upstream and downstream equalize until they converge at level 35. Then, the flow in the dam rises suddenly but decreases proportionately. In this scenario, what happens when the equilibrium of the water levels is reached is not observed, but it is estimated that it will be uniform, becoming almost asymptotic at level 33.

Figure 11 shows the water level before and after the failure versus the abscissa. The abscissa was established from the centre of “Vinces” town to the “Baba” dam. The most affected place is “La Reversa” since a rise of almost 10 m is estimated according to the proposed parameters. Additionally, the town “La Unión” is also affected, with an increase of 4.68 m in the height of the water level.

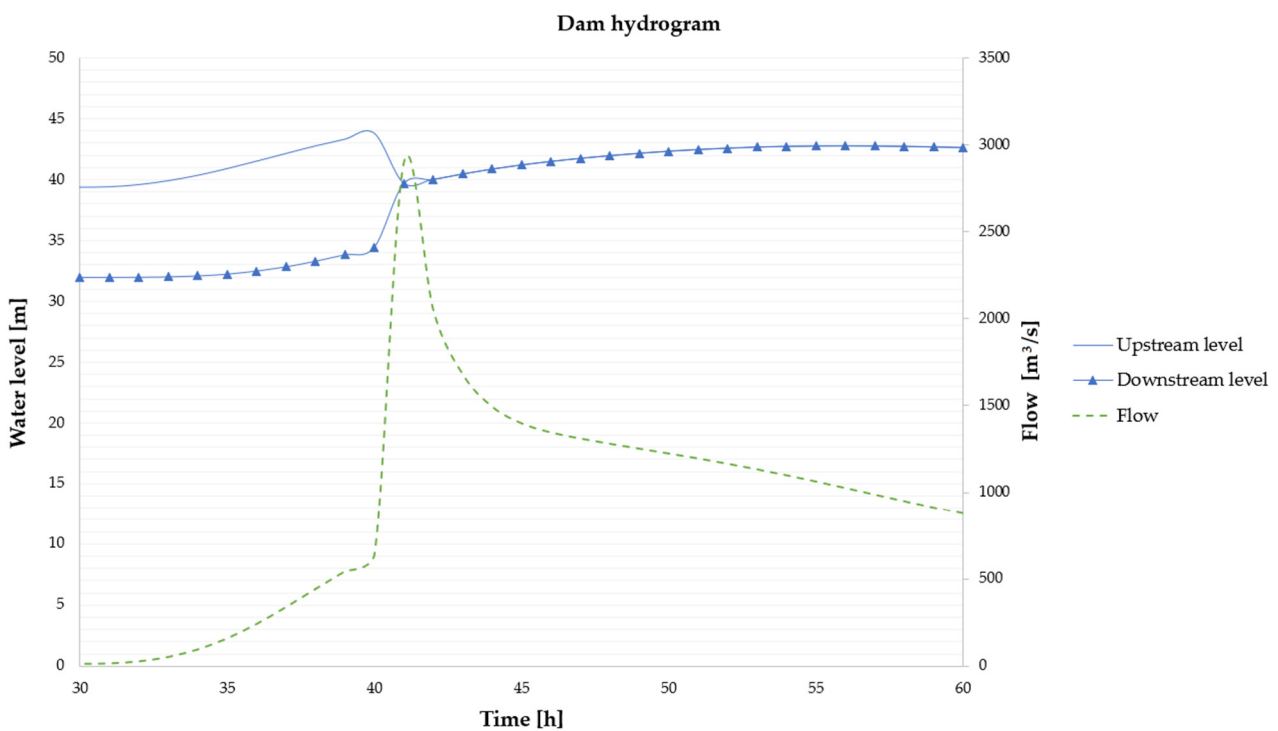


Figure 9. Failure hydrograph scenario A.

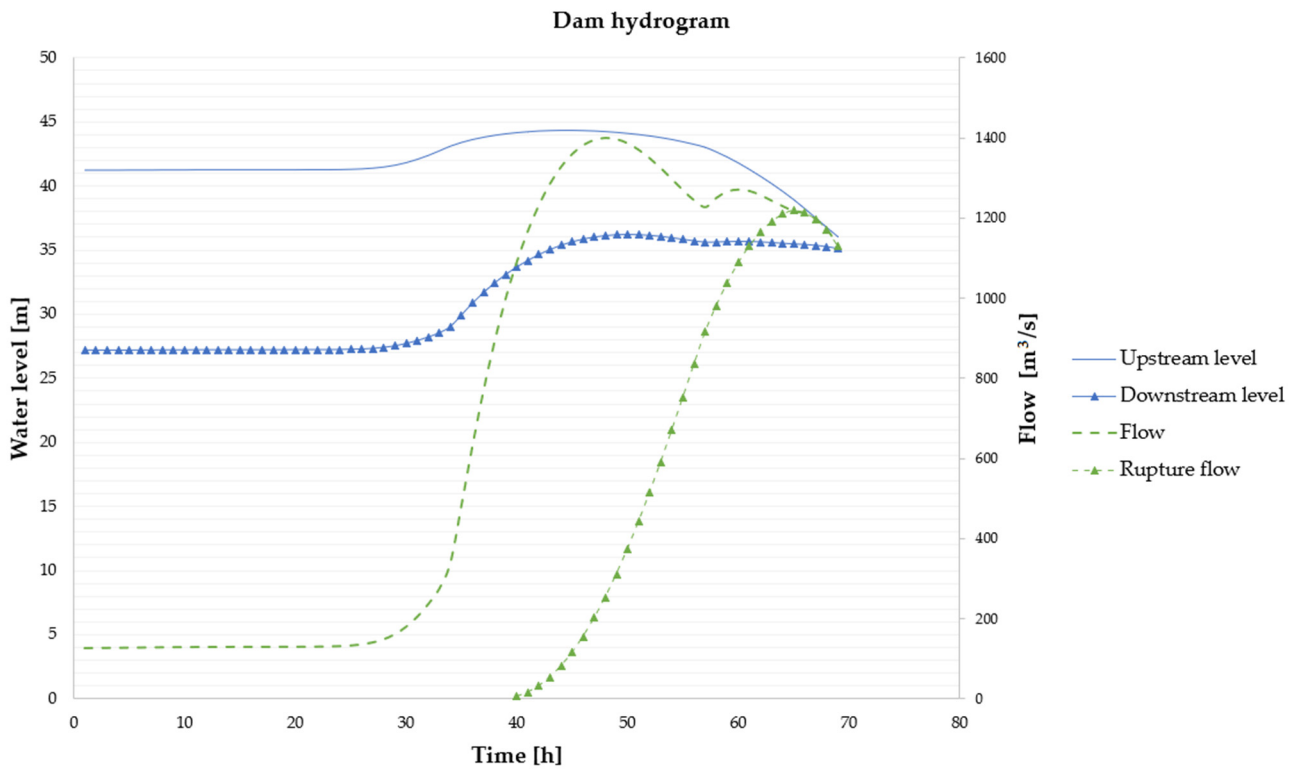


Figure 10. Failure hydrograph scenario B.

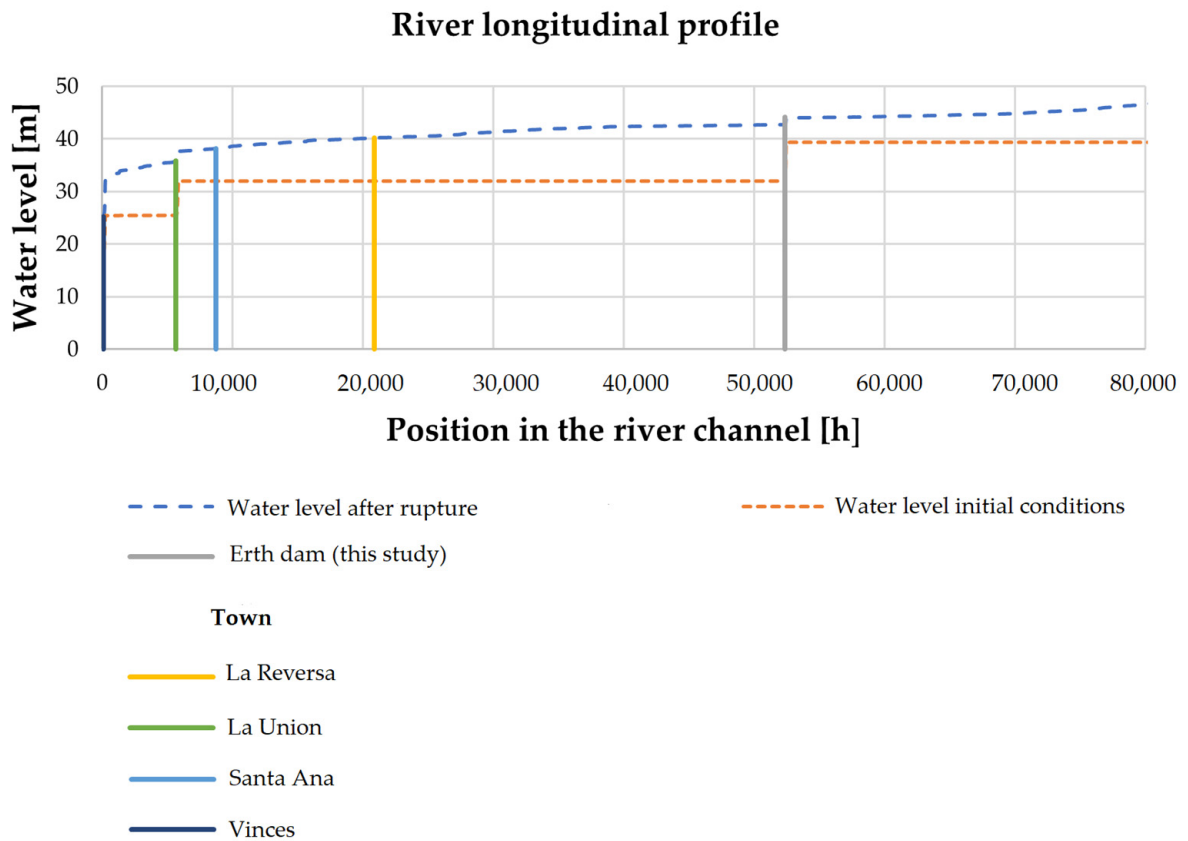


Figure 11. Longitudinal profile of the dam failure.

4.1.8. Verification

The designed dam on the Vincennes River has the dimensions indicated in Table 10, while the spillway dimensions and other considerations are found in Table 11. The berm design was necessary to increase slope stability, and in turn it allowed the saturation line of the flow generated by the filtration to be at a suitable depth. In addition, the upstream berm has the objective of supporting the protective riprap layer.

Table 10. Characteristics of the earth dam.

Parameters	Structure Earth Dam
Height	21 [m]
Width	61 [m]
Altitude	40.77 [m.a.s.l.]
Width of the dam crest	7 [m]
Riprap thickness	1 [m]
Riprap height	1 [m]
Upstream berm level	24.30 [m.a.s.l.]
Downstream berm level	31.13 [m.a.s.l.]
Geomembrane thickness = t_g	2 [mm]
Concrete facing thickness	0.46 [m]

Table 11. Spillway characteristics.

Parameters	Structure Spillway
Height	15 [m]
Width	25 [m]
Altitude	35 [m.a.s.l.]
Spillway length	20 [m]
Access control floor length	8 [m]
Length of sink well	27 [m]
Risberm length	45 [m.a.s.l.]

The concrete facing has a thickness of 0.46 m, enough to cut off the passage of underground flow in the ground. As a watertightness measure for the dam, a geomembrane and geotextile system with a thickness of 2 mm each layer was designed to prevent leaks.

The spillway design is intended to allow excess water to flow without overflowing the dam wall. However, at the end of the spillway rapid there will be a speed that will cause erosion of the land, compromising the structure's safety; thus, it is necessary to design the length of the well or dissipating bowl in order to protect land. Figure 12 presents a three-dimensional view of the designed dam proposed in this investigation.

The dam dimensions verification was carried out by slope stabilization using the GeoStudio 2012 program used in other studies [80–82]. In both cases—without seismic loads and with seismic loads of the upstream slope and downstream slope (Figures 13 and 14)—a safety factor greater than 1.5 was obtained, which means that there is sufficient resistance in the soil in the area to withstand the shear stresses that would cause failures or landslides. In the case of seismic action, the pseudo-static approach was used. This analysis is often used to evaluate the seismic stability of slopes, which consists of applying horizontal and/or vertical inertial body forces [83]. The body dam is assumed to be a rigid element, and

the water body to be of constant density. The gravity acceleration fraction factor (Z) was 0.35, established by the Ecuadorian Construction Standard (NEC acronym in Spanish) [36]. Additionally, the pseudo-static acceleration direction considered in the present study is horizontal, parallel to the flow direction of the dam.

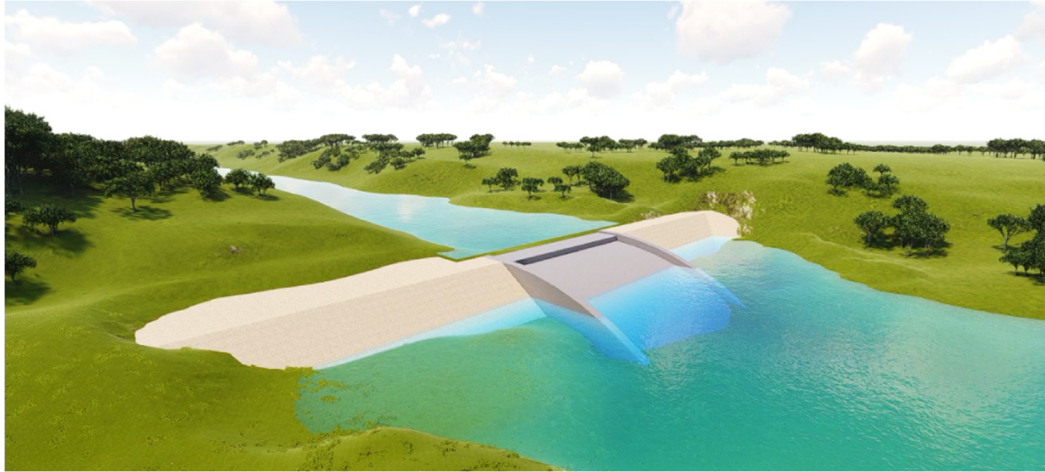


Figure 12. Three-dimensional view of the designed dam.

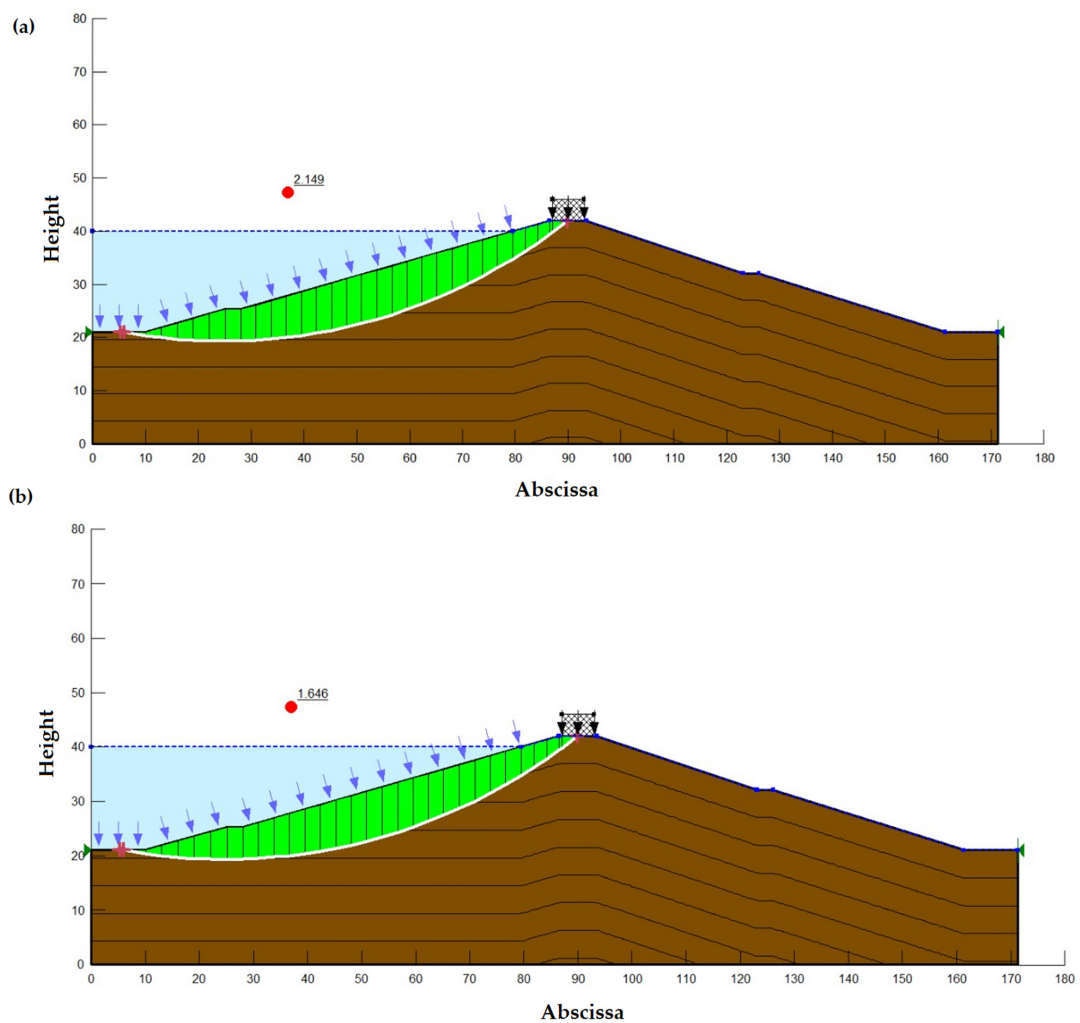


Figure 13. The safety factor of the upstream slope. (a) Slope stabilization with applied loads. (b) Slope stabilization with seismic analysis.

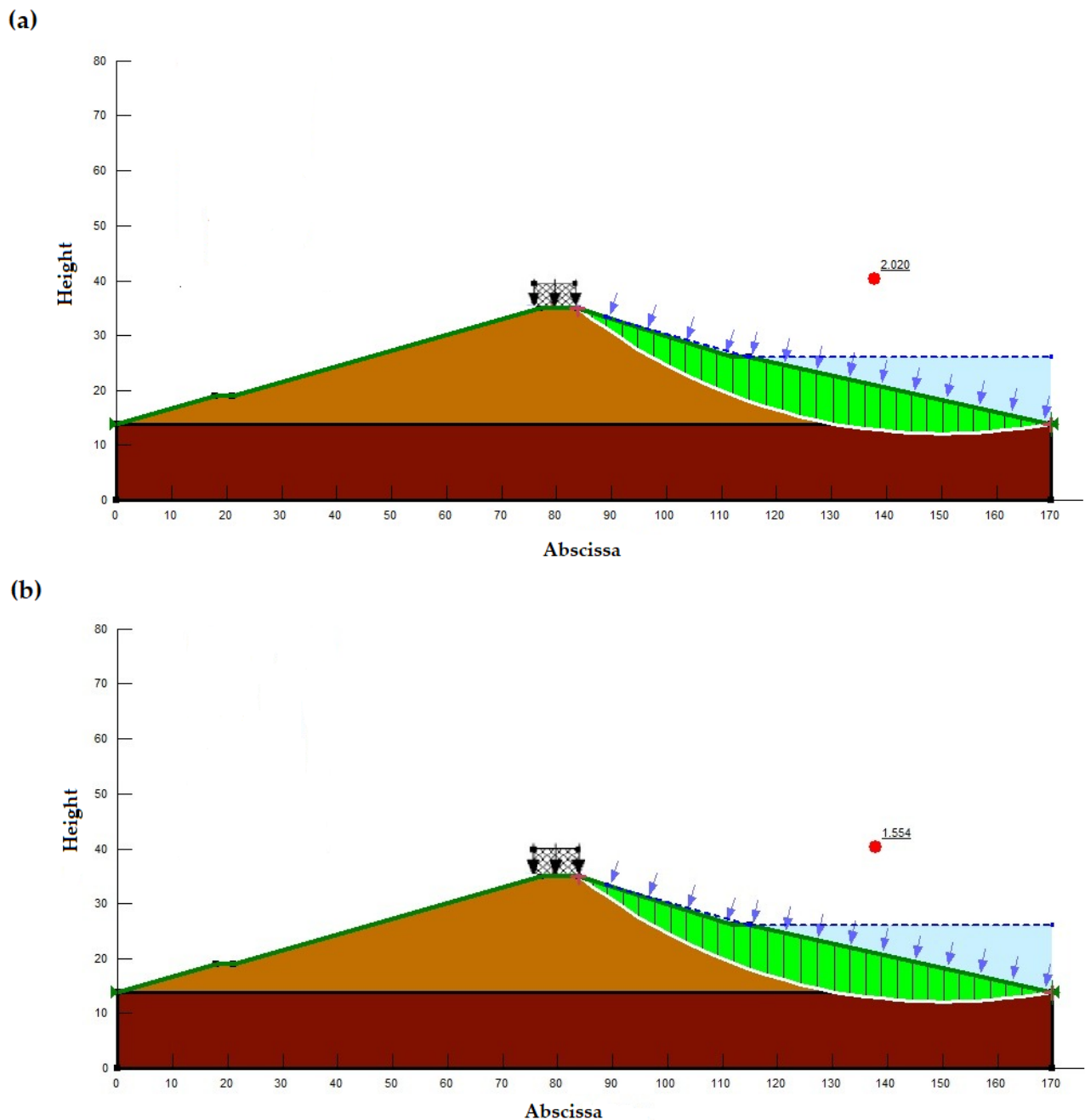


Figure 14. The safety factor of the downstream slope. (a) Slope stabilization with applied loads. (b) Slope stabilization with seismic analysis.

Additionally, the force of the seepage gradient was considered for the dam failure since it is the factor for piping that causes the possibility of solid particles detaching from the soil matrix, which results in corrosion of the dam structure [84,85]. In this earth-fill dam, we contemplate a chimney drain. This structure reduces the pore water pressure inside the embankment and foundation soil. The horizontal filter helps to obtain a lower phreatic line, however, this horizontal drainage causes stratification. The seeping water is carried out efficiently when a vertical filter is added along with the horizontal filter (Figure 15); this implementation will prevent seepage as it will discharge freely.

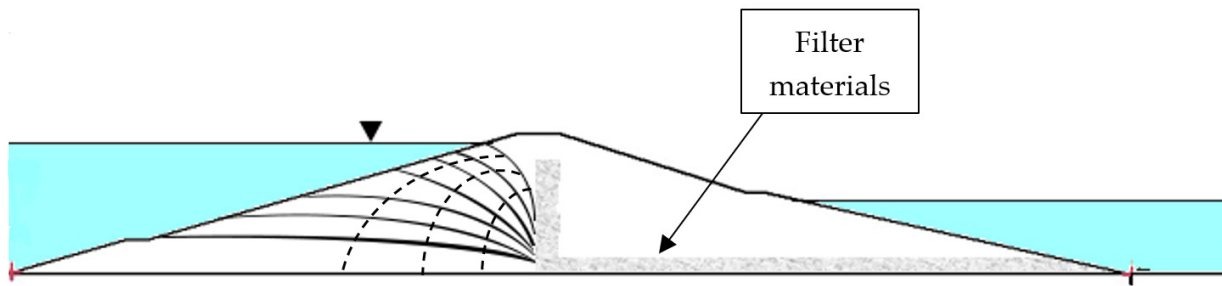


Figure 15. Chimney drain in the proposed earth dam.

4.2. Hydraulic Model Development

Flood Inundation Map

The present study used the HEC-RAS model for the dam breach analysis on the Sara Guerrero site. The results of the dam breach analysis revealed that, in extreme cases, four locations would be affected (Figure 16) in a maximum time of 31 h (Table 12).

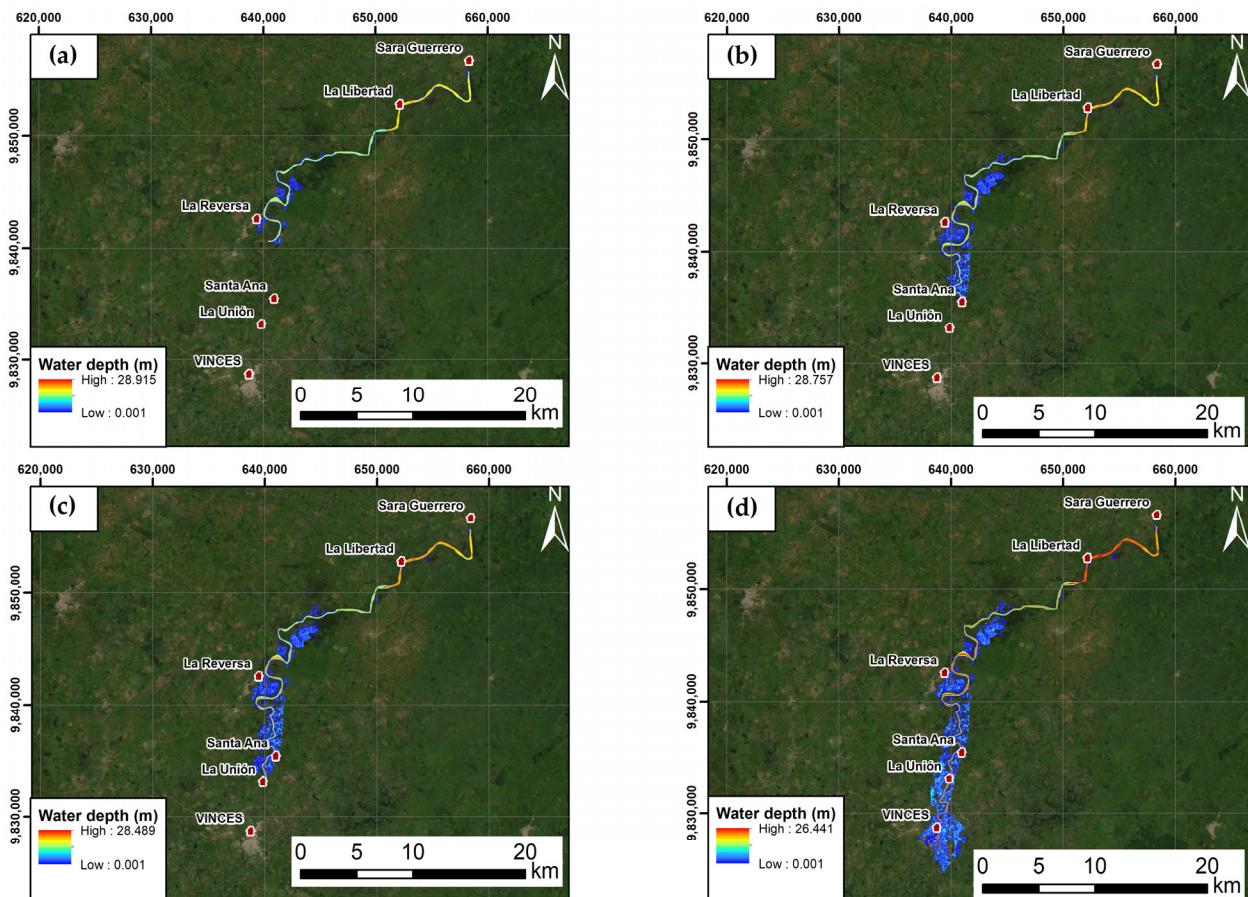


Figure 16. Flood propagation after the dam failure: (a) at 31 h; (b) at 37 h; (c) at 39 h; (d) at 48 h.

Table 12 shows the affected towns, the time the wave arrives, and the distance between the town and the dam. The closest town affected is “La Reversa”, at 31.35 km from the dam, having 31 h to evacuate the area and safeguard human lives. Therefore, the maximum evacuation time available is 48 h, which is enough time for the authorities to create the most suitable plan if they do not have a contingency and evacuation plan. However, due to the conservation of energy and the roughness effect in the channel and plains as the wave

advances, the kinetic energy decreases and so the water level decreases simultaneously (Figure 16).

Table 12. Towns were affected by flood propagation after the dam failure.

Towns	Distance [km]	Time [hours]	Water Level after Failure (m.a.s.l.)	Water Level before Failure (m.a.s.l.)
La Reversa	31.35	31	40.24	32.02
Santa Ana	44.28	37	38.22	32.02
La Unión	46.79	39	35.82	25.50
Vinces	53.40	48	25.26	17.40

5. Conclusions

In this investigation, the type of earth dam near the town “Sara Guerrero” was proposed due to applying the selection criteria of the Likert scale. Based on the results of the design and failure analysis of the dam, the following is concluded:

- (i) The dimensions of the designed dam were verified based on the safety and integrity of the structure through the stability of slopes and seismic conditions.
- (ii) The dam breach analysis encompasses a complex phenomenon where the transfer of the generated flow depends directly on parameters such as terrain roughness, edge conditions, time, and type of failure.
- (iii) The town closest to the dam downstream is “La Libertad”. However, this is not drastically affected by topographical conditions.
- (iv) At 31.35 km after the dam, the first flooded areas are identified, such as the “La Reversa” sector, where the water level rises to 8 m, mainly in considerably depressed sectors.
- (v) In real conditions of a dam failure, the behaviour of the resulting flow will be only an approximation to what is simulated in the software.

In case of failure, the authorities must put together an action plan in the face of an extraordinary event, such as the delimitation of safe access zones and routes for timely evacuation. With the construction of this project, rural areas and towns near the dam implementation area will benefit, protecting the area from flooding and creating collection sources for raw water and irrigation. In general, the construction of a dam generates environmental benefits, reducing annual CO₂ emissions, mitigating climatic phenomena, and aiding the presence of new habitats in the area. However, sometimes negative impacts could occur, so it is necessary to establish clear guidelines for the project to be sustainable, such as soil rehabilitation, slope stability, and gravel and sand traps for maintenance and shock absorbers. (e.g., floodplains) to contain flows in case of exceedance. Decision-makers can use this work to develop land management and emergency plans for the dam if an extraordinary event occurs in the area.

Supplementary Materials: The following supporting information can be downloaded at: <https://www.mdpi.com/article/10.3390/w14132029/s1>, Table S1. Data required for the normal depth [86,87]. Table S2. Slopes for earthen dams. Table S3. Assessment of environmental impacts. Table S4. Prevention/mitigation measures.

Author Contributions: Conceptualization, B.M.-S., J.A.-P., R.A.-R. and M.A.-H.; methodology, B.M.-S., J.A.-P., R.A.-R., P.C.-M., M.J.-M. and M.A.-H.; software, J.A.-P. and R.A.-R.; validation, J.A.-P. and R.A.-R.; formal analysis, B.M.-S., J.A.-P. and R.A.-R.; investigation, B.M.-S., J.A.-P., R.A.-R., P.C.-M., M.J.-M. and M.A.-H.; data curation, J.A.-P. and R.A.-R.; writing—original draft preparation, B.M.-S., J.A.-P., R.A.-R., P.C.-M., M.J.-M. and M.A.-H.; writing—review and editing, B.M.-S., J.A.-P., R.A.-R., P.C.-M., M.J.-M. and M.A.-H.; supervision, B.M.-S. and P.C.-M. All authors have read and agreed to the published version of the manuscript.

Funding: This research received no external funding.

Institutional Review Board Statement: Not applicable.

Informed Consent Statement: Not applicable.

Data Availability Statement: Not applicable.

Acknowledgments: The authors would like to thank researcher Edgar Berrezueta for his help in the review process of this research.

Conflicts of Interest: The authors declare no conflict of interest.

References

1. Wang, P.; Dong, S.; Lassoie, J.P. *The Large Dam Dilemma: An Exploration of the Impacts of Hydro Projects on People and the Environment in China*; Springer: Dordrecht, The Netherlands, 2014; ISBN 9789400776302.
2. Schmutz, S.; Moog, O. Dams: Ecological Impacts and Management. In *Riverine Ecosystem Management*; Springer International Publishing: Cham, Switzerland, 2018; pp. 111–127.
3. Altinbilek, D. The Role of Dams in Development. *Water Sci. Technol.* **2002**, *45*, 169–180. [[CrossRef](#)] [[PubMed](#)]
4. Sayl, K.N.; Muhammad, N.S.; Yaseen, Z.M.; El-shafie, A. Estimation the Physical Variables of Rainwater Harvesting System Using Integrated GIS-Based Remote Sensing Approach. *Water Resour. Manag.* **2016**, *30*, 3299–3313. [[CrossRef](#)]
5. Carrión-Mero, P.; Montalván, F.J.; Morante-Carballo, F.; Loo-Flores de Valgas, C.; Apolo-Masache, B.; Heredia, J. Flow and Transport Numerical Model of a Coastal Aquifer Based on the Hydraulic Importance of a Dyke and Its Impact on Water Quality. Manglaralto—Ecuador. *Water* **2021**, *13*, 443. [[CrossRef](#)]
6. Carrión-Mero, P.; Morante-Carballo, F.; Briones-Bitar, J.; Herrera-Borja, P.; Chávez-Moncayo, M.; Arévalo-Ochoa, J. Design of a Technical-Artisanal Dike for Surface Water Storage and Artificial Recharge of the Manglaralto Coastal Aquifer. Santa Elena Parish, Ecuador. *Int. J. Sustain. Dev. Plan.* **2021**, *16*, 515–523. [[CrossRef](#)]
7. Herrera-Franco, G.; Carrión-Mero, P.; Aguilar-Aguilar, M.; Morante-Carballo, F.; Jaya-Montalvo, M.; Morillo-Balsera, M.C. Groundwater Resilience Assessment in a Communal Coastal Aquifer System. The Case of Manglaralto in Santa Elena, Ecuador. *Sustainability* **2020**, *12*, 8290. [[CrossRef](#)]
8. Carrión-Mero, P.; Morante-Carballo, F.; Vargas-Ormaza, V.; Apolo-Masache, B.; Jaya-Montalvo, M. A Conceptual Socio-Hydrogeological Model Applied to Sustainable Water Management. Case Study of the Valdivia River Basin, Southwestern Ecuador. *Int. J. Sustain. Dev. Plan.* **2021**, *16*, 1275–1285. [[CrossRef](#)]
9. Singh, V.P. *Dam Breach Modeling Technology*; Water Science and Technology Library; Springer: Dordrecht, The Netherlands, 1996; Volume 17, ISBN 978-90-481-4668-0.
10. Charles, J.A.; Tančev, L.; Herschy, R.W.; Cederwall, K.; Gertman, I.; Herschy, R.W.; Herschy, R.W.; Terzhevik, A.; Golosov, S.; et al. *Dam Failures: Impact on Reservoir Safety Legislation in Great Britain*; Bengtsson, L., Herschy, R.W., Fairbridge, R.W., Eds.; Encyclopedia of Earth Sciences Series; Springer: Dordrecht, The Netherlands, 2012; pp. 177–186, ISBN 9781402044106.
11. Goldin, A.L.; Rasskazov, L.N. *Design of Earth Dams*; Zeidler, R.B., Ed.; Routledge: London, UK, 1987; ISBN 9781315141022.
12. Kutzner, C. *Earth and Rockfill Dams: Principles for Design and Construction*; Routledge: London, UK, 2017; ISBN 9780203758991.
13. Titova, T.S.; Longobardi, A.; Akhtyamov, R.G.; Nasyrova, E.S. Lifetime of Earth Dams. *Mag. Civ. Eng.* **2017**, *69*, 34–43. [[CrossRef](#)]
14. Pisaniello, J.D.; McKay, J.M. A Farmer-Friendly Dam Safety Evaluation Procedure as a Key Part of Modern Australian Water Laws. *Water Int.* **2003**, *28*, 90–102. [[CrossRef](#)]
15. Stephens, T. *Manual on Small Earth Dams: A Guide to Siting, Design and Construction*; Food and Agriculture Organization of the United Nations (FAO): Rome, Italy, 2010; ISBN 9789251065471.
16. Sun, Y.; Chang, H.; Miao, Z.; Zhong, D. Solution Method of Overtopping Risk Model for Earth Dams. *Saf. Sci.* **2012**, *50*, 1906–1912. [[CrossRef](#)]
17. Cloete, G.C.; Retief, J.V.; Viljoen, C. A Rational Quantitative Optimal Approach to Dam Safety Risk Reduction. *Civ. Eng. Environ. Syst.* **2016**, *33*, 85–105. [[CrossRef](#)]
18. Shahraki, A.; Zadbar, A.; Motevalli, M.; Aghajani, F. Modeling of Earth Dam Break with SMPDBK Case Study: Bidekan Earth Dam. *World Appl. Sci.* **2012**, *376*–386. [[CrossRef](#)]
19. Urzică, A.; Mihu-Pintilie, A.; Stoleriu, C.C.; Cîmpianu, C.I.; Huțanu, E.; Pricop, C.I.; Grozavu, A. Using 2D HEC-RAS Modeling and Embankment Dam Break Scenario for Assessing the Flood Control Capacity of a Multi-Reservoir System (NE Romania). *Water* **2020**, *13*, 57. [[CrossRef](#)]
20. Albu, L.-M.; Enea, A.; Iosub, M.; Breabăn, I.-G. Dam Breach Size Comparison for Flood Simulations. A HEC-RAS Based, GIS Approach for Drăcșani Lake, Sitna River, Romania. *Water* **2020**, *12*, 1090. [[CrossRef](#)]
21. Brunner, G. *HEC-RAS River Analysis System Hydraulic Reference Manual, Version 5.0*; USACE: Washington, DC, USA, 2016; Volume 547.
22. Brunner, G. *HEC-RAS River Analysis System. Hydraulic User's Manual, Version 6.0*; USACE: Washington, DC, USA, 2021; pp. 456–594.
23. Psomiadis, E.; Tomanis, L.; Kavvadias, A.; Soulis, K.X.; Charizopoulos, N.; Michas, S. Potential Dam Breach Analysis and Flood Wave Risk Assessment Using HEC-RAS and Remote Sensing Data: A Multicriteria Approach. *Water* **2021**, *13*, 364. [[CrossRef](#)]

24. Costabile, P.; Costanzo, C.; Ferraro, D.; Macchione, F.; Petaccia, G. Performances of the New HEC-RAS Version 5 for 2-D Hydrodynamic-Based Rainfall-Runoff Simulations at Basin Scale: Comparison with a State-of-the Art Model. *Water* **2020**, *12*, 2326. [[CrossRef](#)]
25. Zeiger, S.J.; Hubbart, J.A. Measuring and Modeling Event-Based Environmental Flows: An Assessment of HEC-RAS 2D Rain-on-Grid Simulations. *J. Environ. Manag.* **2021**, *285*, 112125. [[CrossRef](#)]
26. Mokhtari, F.; Soltani, S.; Mousavi, S.A. Assessment of Flood Damage on Humans, Infrastructure, and Agriculture in the Ghamsar Watershed Using HEC-FIA Software. *Nat. Hazards Rev.* **2017**, *18*, 04017006. [[CrossRef](#)]
27. Memoria Técnica. Cantón Mocache. Proyecto: Generación de Geoinformación Para La Gestión Del Territorio a Nivel Nacional Escala 1:25,000. Componente 5: “Socioeconómico y Cultural”. 2012. Available online: http://app.sni.gob.ec/sni-link/sni/PDOT/ZONA5/NIVEL_DEL_PDOT_CANTONAL/LOS_RIOS/MOCACHE/IEE/MEMORIAS_TECNICAS/mt_mocache_socioeconomico.pdf (accessed on 10 June 2022).
28. SIPA. Sistema de Información Pública Agropecuaria. Available online: <http://sipa.agricultura.gob.ec/index.php/sipa-estadisticas/estadisticas-productivas> (accessed on 15 July 2021).
29. INEC. Población y Demografía. Available online: <https://www.ecuadorencifras.gob.ec/censo-de-poblacion-y-vivienda/> (accessed on 13 July 2021).
30. Arias-Hidalgo, M.; Villa-Cox, G.; Griensven, A.V.; Solórzano, G.; Villa-Cox, R.; Mynett, A.E.; Debels, P. A Decision Framework for Wetland Management in a River Basin Context: The “Abrás de Mantequilla” Case Study in the Guayas River Basin, Ecuador. *Environ. Sci. Policy* **2013**, *34*, 103–114. [[CrossRef](#)]
31. Ramsar Ramsar Sites Information Service. Available online: <https://rsis.ramsar.org/ris/1023> (accessed on 13 July 2021).
32. SENAGUA. Embalse. Escala 1:250,000. Available online: <http://ide.ambiente.gob.ec/mapainteractivo/> (accessed on 13 July 2021).
33. MAGAP. Cartas Geológicas. Escala 1:100,000. Available online: <https://sni.gob.ec/coberturas> (accessed on 7 June 2021).
34. SNGRE. Geoportal-SNGRE. Available online: <https://srvportal.gestionderiesgos.gob.ec/portal/home/> (accessed on 6 September 2021).
35. INAMHI. Red de Estaciones Meteorológicas e Hidrológicas. Available online: <https://inamhi.wixsite.com/inamhi/novedades> (accessed on 21 September 2021).
36. MIDUVI. Ministerio de Desarrollo Urbano y Vivienda—MIDUVI. Available online: <https://www.habitatyvivienda.gob.ec/documentos-normativos-nec-norma-ecuatoriana-de-la-construccion/> (accessed on 6 September 2021).
37. Zhu, G.; Sang, L.; Zhang, Z.; Sun, Z.; Ma, H.; Liu, Y.; Zhao, K.; Wang, L.; Guo, H. Impact of Landscape Dams on River Water Cycle in Urban and Peri-Urban Areas in the Shiyang River Basin: Evidence Obtained from Hydrogen and Oxygen Isotopes. *J. Hydrol.* **2021**, *602*, 126779. [[CrossRef](#)]
38. Conesa Fernández-Vítora, V.; Conesa Ripoll, L.; Conesa Ripoll, V.; Bolea, E.; Teresa, M.; Ros Garo, V. *Guía Metodológica Para la Evaluación del Impacto Ambiental*; Mundi-Prensa: Madrid, España, 1993.
39. INAMHI. Biblioteca-Instituto Nacional de Meteorología e Hidrología. Available online: <https://www.inamhi.gob.ec/biblioteca/> (accessed on 9 September 2021).
40. Gumbel, E.J. *Statistics of Extremes*; Columbia University Press: New York, NY, USA, 1958; ISBN 9780231891318.
41. Galton, F. The Geometric Mean, in Vital and Social Statistics. *Proc. R. Soc. London* **1879**, *29*, 365–367. [[CrossRef](#)]
42. Pearson, K. Contributions to the Mathematical Theory of Evolution. Skew Variation in Homogeneous Material. *Philos. Trans. R. Soc. Lond.* **1895**, *186*, 343–414. [[CrossRef](#)]
43. Pearson, K. Mathematical Contributions to the Theory of Evolution. Supplement to a Memoir on Skew Variation. *Philos. Trans. R. Soc. Lond. Ser. A Contain. Pap. Math. Phys. Character* **1901**, *197*, 443–459. [[CrossRef](#)]
44. Pearson, K. On the Probable Error of a Coefficient of Mean Square Contingency. *Biometrika* **1915**, *10*, 570. [[CrossRef](#)]
45. Lilliefors, H.W. On the Kolmogorov-Smirnov Test for Normality with Mean and Variance Unknown. *J. Am. Stat. Assoc.* **1967**, *62*, 399–402. [[CrossRef](#)]
46. Chugaev, R.R. *Hydraulic Structures. Part II. Overflow Diversion Dams*; Agropromizdat: Moscow, Russia, 1985. (In Russian)
47. Bakhmeteff, B.A. *Hydraulics of Open Channels*; McGraw-Hill: New York, NY, USA, 1932.
48. Cowan, W.L. Estimating Hydraulic Roughness Coefficients. *Agric. Eng.* **1956**, *37*, 473–475.
49. Burt, R. *Soil Survey Field and Laboratory Methods Manual*; Soil Survey Staff, Ed.; U.S. Department of Agriculture: Washington, DC, USA, 2014.
50. Arcement, G.J.; Schneider, V.R. *Guide for Selecting Manning’s Roughness Coefficients for Natural Channels and Flood Plains United States Geological Survey Water-Supply Paper 2339*; U.S. Geological Survey: Liston, VG, USA, 1989.
51. Likert, R. A Technique for the Measurement of Attitudes. *Arch. Psychol.* **1932**, *140*, 1–22.
52. Pagano, L.; Sica, S. Earthquake Early Warning for Earth Dams: Concepts and Objectives. *Nat. Hazards* **2013**, *66*, 303–318. [[CrossRef](#)]
53. Sandoval, W. *Diseño de Obras Hidrotécnicas*; EDIESPE; Comisión Editorial de la Universidad de las Fuerzas Armadas ESPE: Sangolquí, Ecuador, 2018; ISBN 978-9942-35-390-0.
54. Buldeya, V. *Construcciones Para el Manejo del Agua en Pequeños Ríos (En Ruso)*; Budivelnik: Kiev, Ukraine, 1977.
55. USACE. Gravity Dam Design. In *USACE Engineer Manual*; USACE: Washington, DC, USA, 1995; pp. 1–88, ISBN EM-1110-2-2200.
56. US Bureau of Reclamation. *Design Standards No. 14 Spillways and Outlet Works Design Standard*; US Bureau of Reclamation: Washington, DC, USA, 2014.

57. Gogoaşe Nistoran, D.E.; Gheorghe Popovici, D.A.; Savin, B.A.C.; Armaş, I. GIS for Dam-Break Flooding. Study Area: Bicaz-Izvorul Muntelui (Romania). In *Space and Time Visualisation*; Boştenaru Dan, M., Crăciun, C., Eds.; Springer International Publishing: Cham, Switzerland, 2016; pp. 253–280.
58. Froehlich, D.C. Peak Outflow from Breached Embankment Dam. *J. Water Resour. Plan. Manag.* **1995**, *121*, 90–97. [[CrossRef](#)]
59. Froehlich, D.C. Embankment Dam Breach Parameters and Their Uncertainties. *J. Hydraul. Eng.* **2008**, *134*, 1708–1721. [[CrossRef](#)]
60. Costabile, P.; Costanzo, C.; Ferraro, D.; Barca, P. Is HEC-RAS 2D Accurate Enough for Storm-Event Hazard Assessment? Lessons Learnt from a Benchmarking Study Based on Rain-on-Grid Modelling. *J. Hydrol.* **2021**, *603*, 126962. [[CrossRef](#)]
61. Pasquier, U.; He, Y.; Hooton, S.; Goulden, M.; Hiscock, K.M. An Integrated 1D–2D Hydraulic Modelling Approach to Assess the Sensitivity of a Coastal Region to Compound Flooding Hazard under Climate Change. *Nat. Hazards* **2019**, *98*, 915–937. [[CrossRef](#)]
62. MAGAP. Hidrogeológico. *Escala 1:100,000*. Available online: <http://qa-ide.ambiente.gob.ec:8080/geonetwork/srv/api/records/1535d6a9-57ec-49af-94d3-f2e8e2dc2a43> (accessed on 7 June 2021).
63. Egüez, A.; Alvarado, A.; Yepes, H. Map of Quaternary Faults and Folds of Ecuador and Its Offshore Regions. *US Geol. Surv. Open-File Rep.* **2003**, *3*, 289.
64. de Sherbinin, A.; Castro, M.; Gemenne, F.; Cernea, M.M.; Adamo, S.; Fearnside, P.M.; Krieger, G.; Lahmani, S.; Oliver-Smith, A.; Pankhurst, A.; et al. Preparing for Resettlement Associated with Climate Change. *Science* **2011**, *334*, 456–457. [[CrossRef](#)] [[PubMed](#)]
65. Shi, G.; Zhou, J.; Yu, Q. Resettlement in China. In *Impacts of Large Dams: A Global Assessment*; Tortajada, C., Altinbilek, D., Biswas, A., Eds.; Springer: Berlin/Heidelberg, Germany, 2012; pp. 219–241.
66. Revelo, W. Aspectos Biológicos y Pesqueros de Los Principales Peces Del Sistema Hídrico de La Provincia de Los Ríos, Durante 2009. *Bol. Cient. Téc.* **2010**, *20*, 53–84.
67. Acharya, B.; Joshi, B. Flood Frequency Analysis for an Ungauged Himalayan River Basin Using Different Methods: A Case Study of Modi Khola, Parbat, Nepal. *Meteorol. Hydrol. Water Manag.* **2020**, *8*, 46–51. [[CrossRef](#)]
68. Gil, M.Á.; González-Rodríguez, G. Fuzzy vs. Likert Scale in Statistics. In *Combining Experimentation and Theory. Studies in Fuzziness and Soft Computing*; Trillas, E., Bonissone, P., Magdalena, L., Kacprzyk, J., Eds.; Springer: Berlin/Heidelberg, Germany, 2012; pp. 407–420.
69. Souter, N.; Shaad, K.; Vollmer, D.; Regan, H.; Farrell, T.; Arnaiz, M.; Meynell, P.-J.; Cochrane, T.; Arias, M.; Piman, T.; et al. Using the Freshwater Health Index to Assess Hydropower Development Scenarios in the Sesan, Srepok and Sekong River Basin. *Water* **2020**, *12*, 788. [[CrossRef](#)]
70. Kirshen, P.; Aytur, S.; Hecht, J.; Walker, A.; Burdick, D.; Jones, S.; Fennessey, N.; Bourdeau, R.; Mather, L. Integrated Urban Water Management Applied to Adaptation to Climate Change. *Urban Clim.* **2018**, *24*, 247–263. [[CrossRef](#)]
71. Kittipongvises, S.; Phetrak, A.; Rattanapun, P.; Brundiars, K.; Buizer, J.L.; Melnick, R. AHP-GIS Analysis for Flood Hazard Assessment of the Communities Nearby the World Heritage Site on Ayutthaya Island, Thailand. *Int. J. Disaster Risk Reduct.* **2020**, *48*, 101612. [[CrossRef](#)]
72. Yildiz, A.E.; Dikmen, I.; Birgonul, M.T.; Ercoskun, K.; Alten, S. A Knowledge-Based Risk Mapping Tool for Cost Estimation of International Construction Projects. *Autom. Constr.* **2014**, *43*, 144–155. [[CrossRef](#)]
73. Jamali, A.A.; Ghorbani Kalkhajeh, R. Spatial Modeling Considering Valley's Shape and Rural Satisfaction in Check Dams Site Selection and Water Harvesting in the Watershed. *Water Resour. Manag.* **2020**, *34*, 3331–3344. [[CrossRef](#)]
74. Park, C.; Han, S.; Lee, K.-W.; Lee, Y. Analyzing Drivers of Conflict in Energy Infrastructure Projects: Empirical Case Study of Natural Gas Pipeline Sectors. *Sustainability* **2017**, *9*, 2031. [[CrossRef](#)]
75. MacDonald, T.C.; Langridge-Monopolis, J. Breaching Characteristics of Dam Failures. *J. Hydraul. Eng.* **1984**, *110*, 567–586. [[CrossRef](#)]
76. Evans, S.G. The Maximum Discharge of Outburst Floods Caused by the Breaching of Man-Made and Natural Dams. *Can. Geotech. J.* **1986**, *23*, 385–387. [[CrossRef](#)]
77. Kirkpatrick, J.I.M.; Olbert, A.I. Modelling the Effects of Climate Change on Urban Coastal-Fluvial Flooding. *J. Water Clim. Chang.* **2020**, *11*, 270–288. [[CrossRef](#)]
78. Bharath, A.; Shivapur, A.V.; Hiremath, C.G.; Maddamsetty, R. Dam Break Analysis Using HEC-RAS and HEC-GeoRAS: A Case Study of Hidkal Dam, Karnataka State, India. *Environ. Chall.* **2021**, *5*, 100401. [[CrossRef](#)]
79. Desta, H.B.; Belayneh, M.Z. Dam Breach Analysis: A Case of Gidabo Dam, Southern Ethiopia. *Int. J. Environ. Sci. Technol.* **2021**, *18*, 107–122. [[CrossRef](#)]
80. Hailu, M.B. Modeling Assessment of Seepage and Slope Stability of Dam under Static and Dynamic Conditions of Grindeho Dam in Ethiopia. *Model. Earth Syst. Environ.* **2021**, *7*, 2231–2239. [[CrossRef](#)]
81. Salmasi, F.; Pradhan, B.; Nourani, B. Prediction of the Sliding Type and Critical Factor of Safety in Homogeneous Finite Slopes. *Appl. Water Sci.* **2019**, *9*, 158. [[CrossRef](#)]
82. Shole, D.G.; Belayneh, M.Z. The Effect of Side Slope and Clay Core Shape on the Stability of Embankment Dam: Southern Ethiopia. *Int. J. Environ. Sci. Technol.* **2019**, *16*, 5871–5880. [[CrossRef](#)]
83. Hess, D.M.; Leshchinsky, B.A.; Bunn, M.; Benjamin Mason, H.; Olsen, M.J. A Simplified Three-Dimensional Shallow Landslide Susceptibility Framework Considering Topography and Seismicity. *Landslides* **2017**, *14*, 1677–1697. [[CrossRef](#)]
84. Wang, R.-H.; Li, D.-Q.; Wang, M.-Y.; Liu, Y. Deterministic and Probabilistic Investigations of Piping Occurrence during Tunneling through Spatially Variable Soils. *ASCE-ASME J. Risk Uncertain. Eng. Syst. Part A Civ. Eng.* **2021**, *7*, 04021009. [[CrossRef](#)]

85. Wang, R.-H.; Sun, P.-G.; Li, D.-Q.; Tyagi, A.; Liu, Y. Three-Dimensional Seepage Investigation of Riverside Tunnel Construction Considering Heterogeneous Permeability. *ASCE-ASME J. Risk Uncertain. Eng. Syst. Part A Civ. Eng.* **2021**, *7*, 04021041. [[CrossRef](#)]
86. Nedrigi, V.P. *Designer's Handbook. Hydraulic Structures*; Stroiizdat: Moscow, Russia, 1983. (In Russian)
87. Ministerio de Obras Públicas de España. *Instrucción Para Proyecto, Construcción y Explotación de Grandes Presas*; Ministerio de Obras Públicas de España: Madrid, Spain, 1967.